

Versatile Biological Sample Preparation Platform using Microfluidic
Cell Sorting Device

by
Kyungyong Choi

B.S., Electrical Engineering, Korea Advanced Institute of Science and Technology, 2010

M.S., Electrical Engineering, Korea Advanced Institute of Science and Technology, 2012

Submitted to the Department of Electrical Engineering and Computer Science
in Partial Fulfillment of the Requirements for the Degree of
Doctor of Philosophy

at the

MASSACHUSETTS INSTITUTE OF TECHNOLOGY

September 2021

© 2021 Massachusetts Institute of Technology. All rights reserved

Author

Kyungyong Choi

Department of Electrical Engineering and Computer Science

August 27, 2021

Certified by

Jongyoon Han

Professor of Electrical Engineering and Computer Science

Thesis Supervisor

Accepted by.....

Leslie A. Kolodziejcki

Professor of Electrical Engineering and Computer Science

Chair, Department Committee on Graduate Students

Versatile Biological Sample Preparation Platform using Microfluidic Cell Sorting Device

by
Kyungyong Choi

Submitted to the Department of Electrical Engineering and Computer Science
on August 27 2021 in Partial Fulfillment of the Requirements for the Degree of
Doctor of Philosophy

ABSTRACT

Biological assays for various biological samples are often limited by the low purity of target cells/particles due to the presence of significant host background. A spiral inertial microfluidic cell sorting device can be used to separate cells/particles based on their sizes without any specific labeling and result in a purified sample with a higher purity of target particles, enabling a higher chance of detecting/analyzing those particles of interest for biological assays. Moreover, the cell-sorting ability of spiral devices can be applied as a cell-washing technology to isolate target cells while removing unwanted particles such as adventitious agents for a better quality of cellular products or manufacturing cells in biomanufacturing. This work provides numerous applications of spiral cell sorter-based microfluidic sample preparation on various biological samples. We propose to apply spiral microfluidic sorter for various biological samples to acquire enhanced readouts for targeted downstream assays such as Next-generation sequencing (NGS) or improved quality of cells for biomanufacturing.

Thesis Supervisor: Jongyoon Han

Title: Professor of Electrical Engineering and Biological Engineering

Acknowledgments

I would like to express my gratitude to everyone who has helped me to complete my studies towards the Ph. D. degree at MIT.

First of all, I would like to thank Prof. Jongyoon (Jay) Han for advising me and keeping me inspired for all the research topics during the whole 6 years of my Ph. D. He has always helped me discover scientific findings, even from some frustrating experimental results and has encouraged me to keep on doing research. I learned a lot about how to keep a positive mindset as a researcher and how we contribute to the real world by engaging in research projects from his teaching and doing. I admire and respect his incessant passion, open-mindedness, and curiosity for scientific findings up to this date.

I would also like to thank my thesis committee members, Prof. Joel Voldman and Prof. Paul Blainey for examining my thesis and providing me with valuable feedback with some critical questions for me to answer myself to improve the quality of my thesis.

I am grateful for having such a great group of coworkers and collaborators who have worked together for exciting and engaging research projects during my Ph. D. Although not all of them led to a fruitful ending, a.k.a. publication, I appreciated their help and enjoyed working together. Out of so many names that come to my mind, I would like to specifically mention and thank some of the current and past group members: Hyunryul Ryu, Wei Ouyang, Taehong Kwon, and Hyungkook Jeon as co-authors of papers we have published together. I am also thankful for the current and past members of the Sabeti lab at Broad Institute: Anne Piantadosi, Katherine Siddle, and Lisa Freimark for our successful collaborative project on viral blood preparation and sequencing. I am grateful for having worked for the R01 project with the current and past members of the Hung lab at Broad Institute: Peijun Ma, Jamin Liu, Lorrie He, and Roby Bhattacharyya. I would like to thank some of the Singapore folks at SMART CAMP, CREATE, and SGH who helped me during our collaborative projects in the past: Kelvin Chong, Casandra Tan, Wei Lin Lee, and Yeen Shian Ngow.

I would like to thank all my friends who have filled these seemingly endless years with many joyful memories: Hongjin Jo, '88'-gathering members, Korean EECS cohorts and friends,

Ba-ga families, members of the swimming club and the outdoor activity club at MIT, and members of Rookies from KAIST.

Last but not least, I would like to say I would not have been able to make it towards the end without endless support from my loving family: my mom, grandma, and grandpa, may he rest in peace.

I would like to acknowledge the financial support from Kwanjeong Fellowship, the NIH U24 Sample Sparing assay program (U24-AI118656), the Broadnext10 gift from the Broad Institute (R01AI117043, from NIH), the Singapore MIT Alliance for Research and Technology Antimicrobial Resistance Interdisciplinary Research Group (SMART AMR IRG), and the National Institute for Innovation in Manufacturing Biopharmaceuticals (NIIMBL).

Contents

1	Introduction.....	11
1.1	Emerging need for biological sample preparation methods.....	11
1.2	Trending sample preparation methods using microfluidic devices.....	11
1.3	Spiral inertial microfluidic cell sorter for sample preparation.....	14
2	Improvement on viral recovery and sequencing results by “negative selection” of viral particles from human blood samples.....	16
2.1	Motivation and background.....	16
2.2	Method.....	19
2.2.1	Device fabrication.....	19
2.2.2	Viral blood sample preparation.....	20
2.2.3	Experimental setup for closed-loop operation of the spiral microfluidic device (“C-sep”).....	21
2.2.4	Immunofluorescence staining and flow cytometer analysis.....	21
2.2.5	Extraction and quantification of viral nucleic acid with quantitative polymerase chain reaction (qPCR).....	22
2.2.6	Viral next-generation sequencing (NGS).....	22
2.3	Results and discussion.....	23
2.3.1	Evaluation of spiral microfluidic device performance.....	23
2.3.2	Assessment of virus genome recovery by metagenomic sequencing.....	25
2.4	Chapter conclusion.....	27
3	Clinical human blood sample lysis techniques.....	28
3.1	Motivation and background.....	28
3.2	Method.....	30
3.2.1	Deionized water-based blood lysis.....	30
3.2.2	Red blood cell lysis buffer-based blood lysis.....	31
3.2.3	Saponin-based blood lysis.....	31
3.2.4	Detoxification of saponin.....	31
3.3	Results and Discussion.....	32
3.3.1	Presence of bacteria in blood clots.....	32
3.3.2	Incomplete recovery of bacteria in blood clots by RBC lysis buffer.....	33
3.3.3	Effect of detoxification of saponin.....	34
3.4	Chapter conclusion.....	35

4	Rapid bacteria detection from blood samples without culture or PCR.....	36
4.1	Motivation and background.....	36
4.2	Method.....	39
4.2.1	Fabrication of microfluidic devices.....	39
4.2.2	Preparation of bacteria-spiked blood samples.....	39
4.2.3	Process workflow.....	40
4.3	Results and discussion.....	41
4.3.1	Evaluation of spiral cell sorter performance.....	41
4.3.2	Evaluation of electrokinetic concentrator performance.....	42
4.3.3	Evaluation of detection sensitivity and specificity.....	43
4.4	Chapter conclusion.....	44
5	Scalable and Continuous Cell Washing Method by Spiral Inertial Microfluidics for Adventitious Agent Clearance.....	45
5.1	Motivation and background.....	45
5.2	Method.....	49
5.2.1	Fabrication of spiral microfluidic cell sorter.....	49
5.2.2	Preparation of CHO cell culture.....	49
5.2.3	Preparation of fluorescent beads, bacteria, and virus-spiked samples and characterization of clearance.....	50
5.2.4	Continuous cell washing by constant medium addition.....	51
5.2.5	Neuraminidase treatment.....	51
5.2.6	Evaluation of spiral microfluidic cell sorter performance.....	52
5.3	Results and Discussion.....	52
5.3.1	Evaluation of cell washing efficiency for plastic bead clearance.....	53
5.3.2	Evaluation of cell washing efficiency for bacterial clearance.....	54
5.3.3	Evaluation of cell washing efficiency for viral clearance.....	55
5.3.4	Area of Application for Spiral-based Cell Washing Technology.....	57
5.3.5	Comparison with Currently Available Technology.....	58
5.4	Chapter conclusion.....	59
6	Conclusion and Outlook.....	60
	Bibliography.....	62

List of Figures

Figure 1 Bright-field image and schematic of lab-on-a-disc platform microfluidic device for blood sample preparation.....	12
Figure 2 Schematic and frames from a movie of digital microfluidics for human blood sample preparation.....	13
Figure 3 Examples of other microfluidic approaches for sample preparation.....	14
Figure 4 Schematic and photographs of the experimental setup for closed-loop separation spiral microfluidic device with a negative selection scheme.....	19
Figure 5 Characterization of open-loop spiral cell sorting operation on whole blood and plasma samples at different dilutions.....	21
Figure 6 Evaluation of host cell removal and virus recovery after closed-loop spiral cell sorting operation with a negative selection scheme.....	25
Figure 7 Metagenomic sequencing results for comparison between untreated and spiral microfluidics-processed samples.....	27
Figure 8 Schematic of bacteria entrapment in blood clot and discharge of them by blood lysis.....	30
Figure 9 Schematic of pressure-modulated selective electrokinetic trapping (PM-SET) principle.....	37
Figure 10 Overall flow chart of our microfluidic platform for the separation and detection of bacteria from a blood sample.....	39
Figure 11 Schematic and microscope images of spiral microfluidic sorter operation for separation of bacteria from blood.....	41
Figure 12 Schematic and photographs of experimental setup and characterization of spiral cell sorting performance on host blood cell removal and bacteria recovery.....	42
Figure 13 Schematic and characterization of two-stage 640-plex electrokinetic concentrator.....	43

Figure 14 Evaluation of bacteria detection sensitivity and specificity using a two-stage electrokinetic concentrator.....	43
Figure 15 Constant medium addition scheme of spiral microfluidic sorter operation for cell washing.....	48
Figure 16 Evaluation of spiral sorter-based cell washing performance on 1- μ m beads removal and CHO cell recovery.....	53
Figure 17 Evaluation of spiral sorter-based cell washing performance on bacteria removal and CHO cell recovery.....	55
Figure 18 Evaluation of spiral sorter-based cell washing performance on virus removal and CHO cell recovery.....	56

List of Tables

Table 1 Comparison of bacteria quantity between unlysed and lysed blood samples.....	33
Table 2 Comparison of viable bacteria recovery from samples lysed by RBC lysis buffer and DIW.....	34
Table 3 Comparison of viable bacteria recovery after applying three different blood lysis methods (DIW, saponin, detoxified saponin).....	34

Chapter 1

Introduction

1.1 Emerging need for biological sample preparation methods

As many researchers in the biology or biological engineering field are interested in analyzing more diverse and difficult-to-treat biological samples, the need for proper sample preparation has arisen.^{1,2} These biological samples include whole blood, plasma³, sputum⁴, pus⁵, *etc.* It is usually challenging to acquire biological assays of fair quality on these samples due to the abundance of background host cells such as red blood cells, white blood cells, and platelets for whole blood and plasma samples, presence of intrinsic biological/chemical barrier such as mucus for sputum, or debris of dead immune cells for pus. Also, most of these samples may display very different characteristics such as different viscosity for sputa samples or different cell concentrations for blood samples depending on the severity of the disease or patients. Therefore, a sample preparation method that can purify/isolate target cells, nucleic acids, or proteins of interest, regardless of sample conditions, is required to enhance the quality of the downstream biological assay. Moreover, the sensitivity of the assay can be significantly enhanced by the reduction of unnecessary background cells with proper sample preparation so that it enables researchers to observe the results that have been regarded as unable to be observed.⁶

1.2 Trending sample preparation methods using microfluidic devices

It would be of much help for researchers who seek to perform biological assays on the aforementioned biological samples if we provide a method to properly prepare those samples. That is why many research groups have developed various kinds of microfluidic devices to help

prepare biological samples of interest.

Some groups have adopted a “lab-on-a-disc” platform to use the centrifugal force caused by the controlled rotational motion of the micro-structured disc on a spinner.^{7–9} With the help of centrifugal force, blood cells or antibody-coated beads for a target biological assay (*i.e.*, enzyme-linked immunosorbent assay (ELISA)) were pelleted down for extraction of plasma or target particles attached to the bead and transport of the reagents required for the delivery of target particles were manipulated (Figure 1).

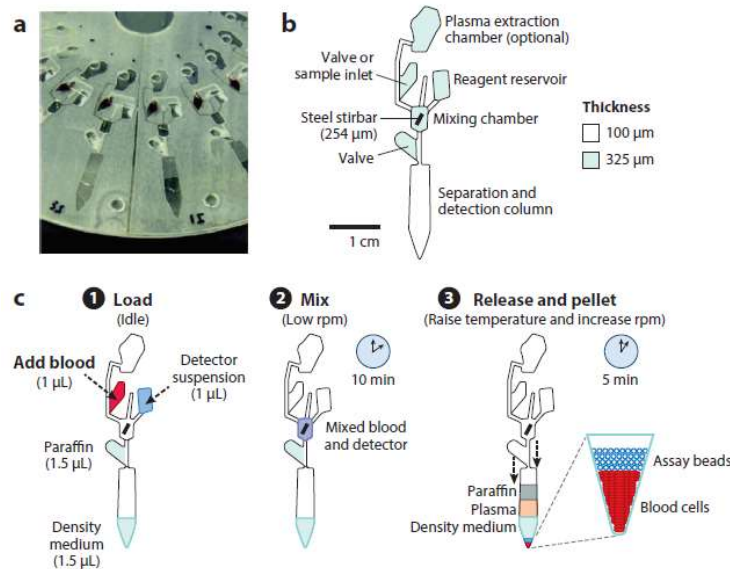


Figure 19 Bright-field image and schematic of lab-on-a-disc platform microfluidic device for blood sample preparation⁷. Figures are reprinted by permissions from Oxford University Press, copyright (2011)

The “Digital microfluidics” platform was chosen by other research groups where the motion of individual droplets in confined micro-structure can be controlled under the principle of electrowetting by actuating selected arrays of electrodes underneath the droplet (Figure 2).^{10–13} Human physiological fluid samples such as serum, plasma, urine, and saliva were transported on the digital microfluidic system and tested for colorimetric enzymatic glucose assay by Srinivasan *et al.*¹⁰ Wheeler *et al.* demonstrated sample preparation on a digital microfluidics platform for Matrix-Assisted Laser Desorption/Ionization Mass Spectrometry (MALDI-MS) by transporting droplets which contain proteins or peptides and matrix to the specific location of the device.¹¹ Chang *et al.* performed polymerase chain reaction (PCR) on a digital microfluidics platform

utilizing sample transportation and mixing ability of the platform¹², and Mousa *et al.* developed an estrogen assay on a digital microfluidic platform where estrogen in breast tissue homogenate, whole blood, and serum can be extracted and measured by mass spectrometry¹³.

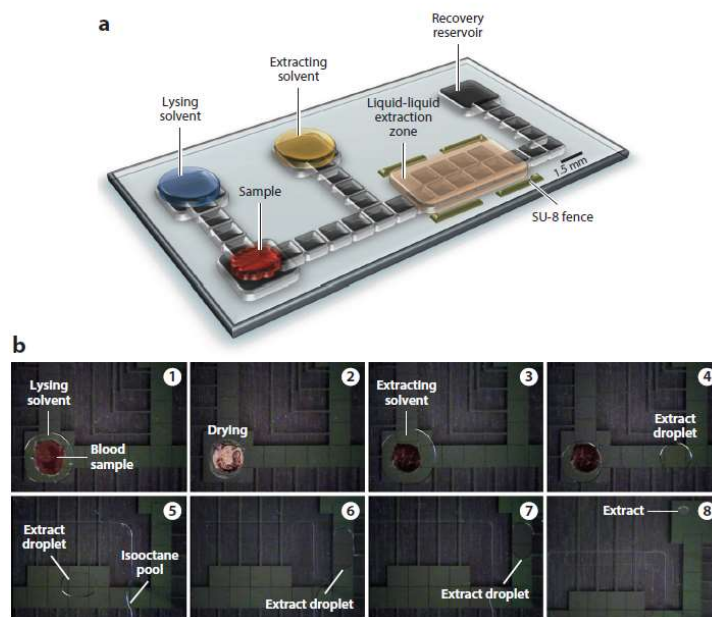


Figure 20 Schematic and frames from a movie of digital microfluidics for human blood sample preparation.¹³ Figures are reprinted by permissions from The American Association for the Advancement of Science, copyright (2009)

Other microfluidic approaches for biological sample preparation include, but are not limited to, sedimentation- and capillary-assisted platforms^{14,15} (Figure 3.A and B) and magnetophoresis-assisted devices^{16–19} (Figure 3.C). Zhang *et al.* devised a microfluidic platform where the plasma of a blood sample is continuously separated by the natural aggregation and sedimentation behavior of red blood cells.¹⁵ In a magnetophoresis-assisted microfluidic platform developed by Pamme *et al.*, continuous separation of mouse macrophage and human ovarian cancer cells (HeLa) were enabled by attaching magnetic nanoparticles to them where a magnetic field was applied to deflect target cells' passage toward different outlets.¹⁷

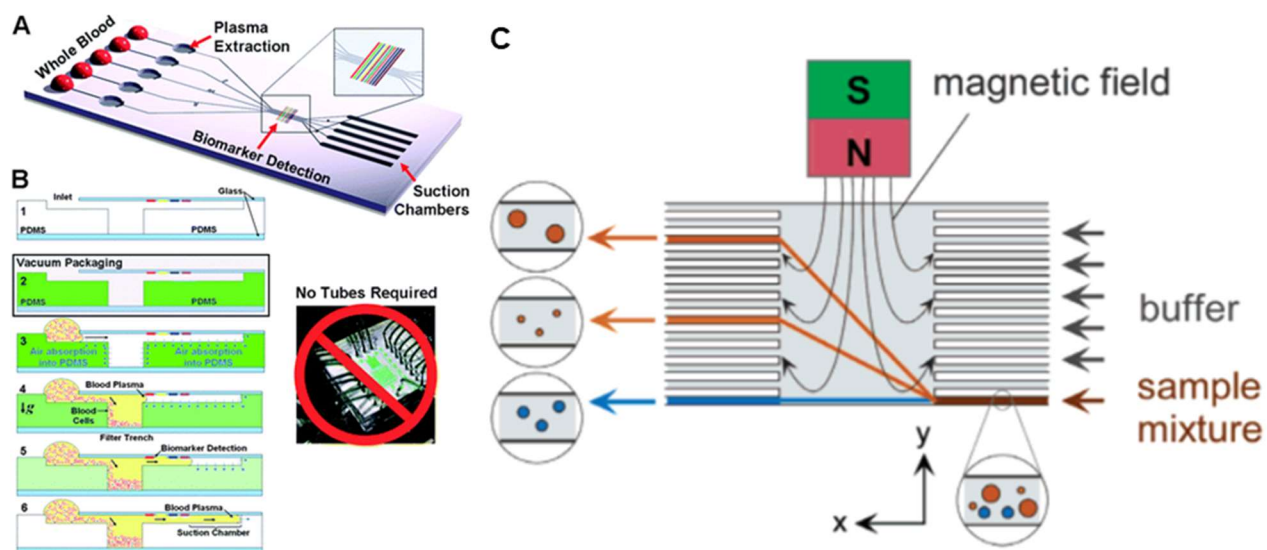


Figure 21 (A),(B) Schematic of sedimentation- and capillary-assisted microfluidic device for plasma extraction from a blood sample.¹⁴ (Dimov et al., Lab Chip 2011, 11, 845-850, Reproduced by permission of The Royal Society of Chemistry) (C) Conceptual schematic of the magnetophoresis-assisted microfluidic particle separation device.¹⁶ Reprinted with permission from (Pamme et al., Anal. Chem. 2004, 76, 7250-7256). Copyright (2004) American Chemical Society

1.3 Spiral inertial microfluidic cell sorter for sample preparation

Spiral inertial microfluidic device has been widely used on various biological sample preparation to separate cells according to their sizes in a label-free manner.^{3,4,20–24} Cells of different sizes locate themselves in different locations in a spiral microchannel due to the combined effect of inertial net lift force ($F_L \propto a_p^4$, a_p : particle diameter) caused by the inertia of the particle suspended in a Poiseuille flow and Dean drag force ($F_D \propto a_p$) caused by Dean vortex formed in a curved microchannel.²⁰ Larger cells, primarily affected by the net lift force, tend to be focused near the inner-wall side of the microchannel, while smaller cells are dominated by the Dean drag and dispersed throughout the microchannel.

Spiral microfluidic cell sorter takes advantage of this feature and separates cells in a biological sample based on their sizes. It has advantages over other microfluidic approaches such as blood cell sedimentation,^{14,15} membrane-based filtration,^{25,26} on-chip centrifugation,^{27,28} cross-flow filtration^{29–31} in that it can be operated continuously at high throughput without clogging or filter/membrane fouling, regardless of the sample volume. The spiral microfluidic sorter also shows robust particle separation performance for samples with diverse physical properties with a

proper amount of dilution. Furthermore, spiral microfluidic cell sorter benefits the end-user of the processed biological samples because it minimizes disruption on the target cells caused by chemical/biological modifications of cell receptors, affecting the viability or gene expression of the target cells.

However, there exist two main bottlenecks that limit the applicability of spiral microfluidic sorter on real-world samples: 1) It is challenging to focus small cells with inertial net lift force, and it results in low recovery of them; 2) It requires high dilution for samples with high solid volume fraction (*e.g.*, blood) to prevent particle-particle interaction and enable proper particle focusing in the microchannel, which results in undesirable, large processed sample volume. We propose a new operational scheme of spiral microfluidic sorter called negative selection with recirculatory feedback to achieve high recovery and purity of small bio-particles such as bacteria and nucleic acids and connect this device with a proper method of concentration to reduce the final processed volume as well.

Chapter 2

Improvement on viral recovery and sequencing results by “negative selection” of viral particles from human blood samples¹

2.1 Motivation and background

Isolation of viral nucleic acid from human clinical samples is important in the diagnosis of many infectious diseases and also represents the critical first step in scientific studies of viral genomics and pathogenesis. Recently, metagenomic sequencing has become a prominent method for virus detection^{32,33}, discovery^{34–37}, and viral genome sequencing for studies of evolution and pathogenesis^{38,39}. In this technique, all DNA, RNA, or total nucleic acid in a sample is sequenced in an unbiased fashion, and computational algorithms are used to recover the viral sequencing reads of interest. The major advantage of this technique is that it is a flexible methodology that can be applied to any virus, including settings in which the pathogen may be unknown or novel. However, a substantial limitation is the recovery of sequencing reads from the human host,

¹ *The following published journal paper was used in its entirety for Chapter 2, with minor updates and modifications:*

Choi, K.; Ryu, H.; Siddle, K. J.; Piantadosi, A.; Freimark, L.; Park, D. J.; Sabeti, P.; Han, J. Negative Selection by Spiral Inertial Microfluidics Improves Viral Recovery and Sequencing from Blood. *Anal. Chem.* **2018**, *90* (7), 4657–4662.

Contributions: K.C., K.S., A.P., P.S. and J.H. conceived of the approach and designed the experiments. K.C. and H.R. designed and fabricated the spiral microfluidic sorter device and conceived of the “negative selection” operational scheme of the spiral microfluidic sorter. K.C., K.S., A.P. and L.F. executed experiments on viral blood sample preparation. K.C. executed immunofluorescence staining and flow cytometer analysis. K.S., A.P., and L.F. executed extraction and quantification of viral nucleic acid with quantitative polymerase chain reaction (qPCR). K.S., A.P., and D.J.P. contributed to the analysis of sequenced results from viral next-generation sequencing. K.C., K.S., A.P., L.F. and J.H. mainly drafted the manuscript which all authors have read and approved.

which vastly outnumbers viral sequencing reads even in low-cell-content fluids like plasma and cerebrospinal fluid. This leads to costly high-depth sequencing and limits the recovery of reads from low abundance viruses. This has prompted the development of host-depletion methods such as selective removal of human ribosomal RNA^{40,41}. However, this is less useful in detecting and sequencing DNA viruses where the background from host DNA remains.

Microfluidic isolation of viral particles and free nucleic acid offers an opportunity to enhance detection of both RNA viruses and DNA viruses, and importantly can be performed directly from whole blood, eliminating the need for centrifugation and perhaps enhancing the detection of some viruses (*e.g.*, West Nile Virus) that adhere to red blood cells^{42,43}. Earlier microfluidic devices implemented capillary imbibition^{44,45}, blood cell sedimentation^{14,15}, cross-flow filtration²⁹⁻³¹, on-chip centrifugation^{27,28}, and membrane-based filtration^{25,26}. These various applications were limited by non-continuous operation, low throughput, or small sample volume, and clogging and fouling of filter/membrane. Shim *et al.*⁴⁴ and Lee *et al.*⁴⁵ developed micro-channel structures that are either packed or coated with micro/nano-sized silica beads to induce a capillary plasma extraction from whole blood. Dimov *et al.*¹⁴ demonstrated a self-powered integrated microfluidic platform in which plasma is separated by natural sedimentation inside the microfluidic channel while the sample transport is propelled by the self-contained vacuum in the channel. VanDelinder *et al.*³⁰ devised a microfluidic device that can separate plasma from diluted whole blood by size exclusion in a cross-flow. Haeberle *et al.*²⁷ presented a centrifugation-based microfluidic device on a disc that enables plasma extraction from whole blood by carefully manipulating centrifugal force to transport the blood as well as to sediment the cellular pellet and to decant the plasma inside the device structure. Researchers have adopted membrane-based microfluidic devices to extract plasma from whole blood samples spiked with viruses or drawn from virus-infected patients and successfully recovered sufficient virus to be quantified with a viral load test.^{25,26} Wang *et al.*²⁶ fabricated a filter-based lab-on-a-chip device that can isolate plasma as well as viruses from unprocessed whole blood and reported viral recovery of 73-83%. Liu *et al.*²⁵ also demonstrated a membrane-based plasma separating device that is facilitated by gravitational sedimentation and were able to recover 82-96% of HIV virus from multiple load samples. Recently, inertial microfluidics, which can separate particles based on their sizes by utilizing and balancing forces inside the micro-channel, have been spotlighted as an alternative to

prepare biological samples in a continuous, high-throughput, non-clogging manner before further downstream assays.^{4,22,46-51} Rafeie *et al.*⁵¹ presented a high-throughput slanted spiral microchannel device that can extract plasma from diluted whole blood from small to large volume (1-100mL) with a maximum processing flow rate of 24 mL/min. However, the performance of inertial microfluidics is often limited by the conventional single-pass operation, which results in an intrinsic trade-off between purity and recovery when the window of optimal operation is narrow.

As an effort to remedy this issue of single-pass operation, our group introduced a closed-loop operation of the spiral microfluidic device, called “C-sep,” where both enrichment and recovery of target cells can be maximized by continuously feeding the inertially focused stream of target cells back to the input.⁴

In this chapter, we present a simple microfluidic sample preparation method using a spiral microchannel device, resulting in enhanced detection of virus from blood samples using unbiased metagenomic sequencing. To our best knowledge, this is the first time to demonstrate a whole workflow from microfluidic sample preparation to metagenomic sequencing-based virus detection. Our spiral inertial microfluidic device is operated in a recirculatory regime so that virus can be isolated via negative selection from the diluted blood while large host cells are kept in the recirculating flow. Conventionally, it has been considered challenging to isolate small particles like viruses (a few tens or hundreds of nanometers) with an inertial microfluidic device because these small particles are prone to Brownian motion and are too small to be inertially focused with the net lift force in a microchannel.⁵² We separate viruses from the host cells—red blood cells (RBC), white blood cells (WBC), and platelets—by keeping the host cells (larger than or equal to 3 μm in diameter) focused in the closed-loop while collecting the outer-wall output which mainly consists of free-floating viruses in background fluid, along with cell-free nucleic acid. In this manner, negatively selected viral particles can be collected with the buffer solution, with most of the host cells depleted in an automated and fully contained manner (Fig. 4 A). The utility of spiral microfluidics with a negative selection scheme was verified by processing whole blood samples spiked with cytomegalovirus (CMV), analyzing the resulting suspension with quantitative PCR and viral sequencing, and comparing the results between

treated and untreated samples. We observed a significant increase in the number of viral reads as well as viral genome coverage depth for microfluidics-treated samples. The increase in viral reads was higher in samples with low virus concentration, which suggests the potential for using our device and operation scheme for pre-treatment of clinical whole blood samples.

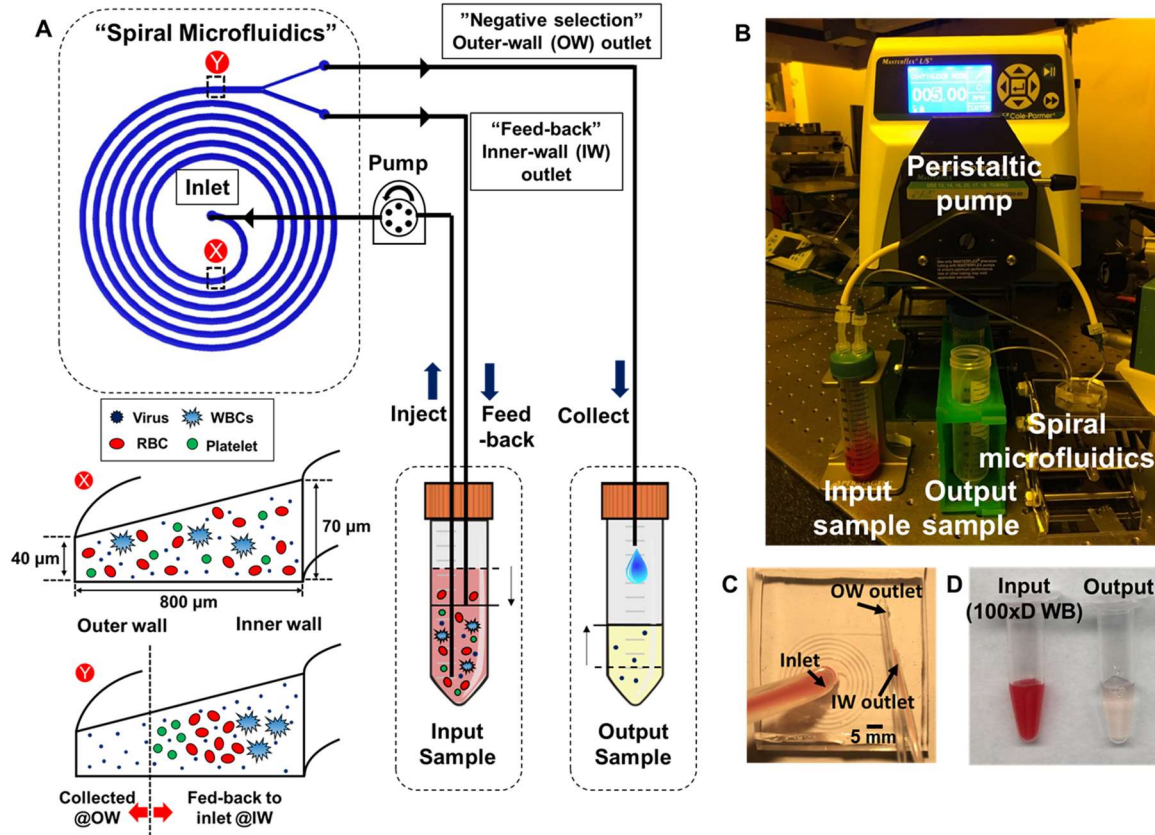


Figure 22 (A) Schematic of closed-loop separation (“C-sep”) spiral microfluidic device platform with negative selection scheme (B) Photograph of the experimental setup (C) Magnified view of spiral microfluidic device (D) Comparison between input (100 times diluted whole blood) and microfluidics (MF)-treated samples

2.2 Method

2.2.1 Device fabrication

The spiral inertial microfluidic device was fabricated with polydimethylsiloxane (PDMS) following standard soft-lithographic microfabrication techniques as described previously.⁴ The master mold with specific microchannel dimensions was designed with AutoCAD software and then fabricated with a micro-milling machine (Whits Technologies,

Singapore) on aluminum. PDMS replica was fabricated by casting degassed PDMS (10:1 mixture of base and curing agent of Sylgard 184, Dow corning Inc.) onto the aluminum mold, curing on the hot plate for 10 minutes at 150 degrees, and peeling the cured PDMS off the mold. Holes for fluidic access were punched with disposable biopsy punches (Integra™ Miltex®). The punched PDMS replica was then irreversibly bonded to a silicone film (BISCO HT-6240 40 Duro silicone sheet, 0.25mm-thick, Rogers Corp.) placed on a glass slide after treating both surfaces with a plasma machine (Femto Science, Korea). The assembled device was placed in a 60 degrees oven for 1 hour to stabilize the bonding further.

2.2.2 Viral blood sample preparation

Fresh human whole blood samples collected in an ethylenediaminetetraacetic acid (EDTA) vacutainer (purple top) were purchased from Research Blood Components, LLC (Boston, MA, USA) and spiked with known concentrations of cytomegalovirus (ATCC-2011-8) to generate samples representing a range of clinically-relevant viral loads (10^4 - 10^8 CMV copies/mL whole blood). Plasma samples were prepared by centrifugation of whole blood for 10 minutes at 994 RCF, followed by the collection of the plasma layer. As a control, some plasma samples underwent lysis of cell and viral membranes by combining 200 μ L of plasma samples with 800 μ L of buffer AVL (Qiagen).

In preparation for loading in the spiral microfluidic device, samples were diluted in buffer comprised of phosphate-buffered saline without calcium and magnesium (PBS, Corning®) plus 0.1% w.t. bovine serum albumin (BSA, Sigma-Aldrich) to prevent non-specific binding of cells and viral particles to device surface and tubing. Whole blood samples were diluted 100-fold (100 μ L whole blood in 9,900 μ L buffer), and plasma samples were diluted 10-fold (1 mL plasma in 9 mL buffer). Due to differences in the number of host cells, different dilution factors were chosen for whole blood and plasma samples to yield the best rejection ratio of host cells (Fig. 5).

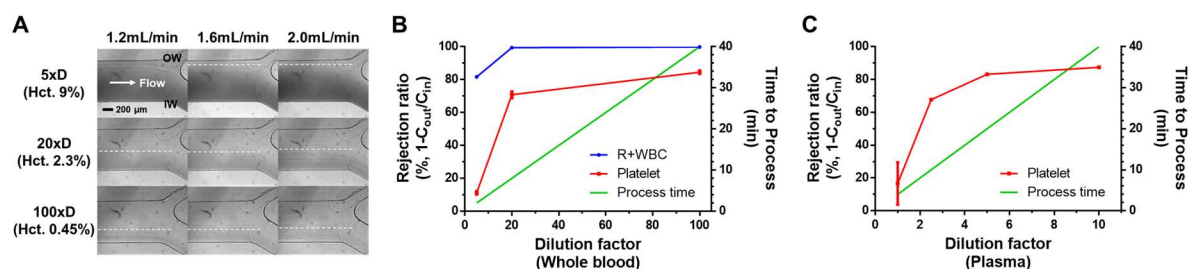


Figure 23 (A) Microscopic images of inertial focusing behavior in whole blood samples at different dilution and flow rates. (B) Rejection ratio of host cells in outer-wall (OW) output samples for whole blood samples at different dilutions. The rejection ratio was calculated by how much concentration of host cells in the outer-wall (OW) output is reduced compared to the input. (C) Rejection ratio of host cells in outer-wall (OW) output samples for plasma samples at different dilutions

2.2.3 Experimental setup for closed-loop operation of the spiral microfluidic device (“C-sep”)

Closed-loop operation of spiral inertial microfluidic device was done by connecting a peristaltic pump (Cole-Parmer) to the device with silicone tubing (Masterflex platinum-cured tubing, L/S 14, Cole-Parmer) with sample tubes (Falcon® Polystyrene Sterile Centrifuge Tubes, Corning®) loaded on a rack (Fig. 4 B). Tubing connected to the inner-wall side outlet was fed back to the input tube for closed-loop operation while the output sample was being collected at the outer-wall side outlet tubing. This operation was continued until all input volume was processed with the optimized flow rate of 1.6 mL/min (Fig. 5 A).

2.2.4 Immunofluorescence staining and flow cytometer analysis

All input and output samples were aliquoted in a volume of 100 μL and stained with 10 μL of allophycocyanin (APC)-conjugated mouse antihuman CD41a reagent (Miltenyi Biotec) for 30 minutes at 4 degrees in the dark. The stained samples were then analyzed by BD Accuri C6 flow cytometer (BD Bioscience) to quantify the number of RBC/WBCs/platelets in each sample based on the number of events gated by fluorescence intensity, forward-scattering, and side-scattering, accordingly. To evaluate how much cell fraction was removed from the input to the output, we recorded the volume of each input and output sample and multiplied these volumes by the number of events per processed

sample volume in the aliquoted samples to calculate the total number of each cell type.

2.2.5 Extraction and quantification of viral nucleic acid with quantitative polymerase chain reaction (qPCR)

Nucleic acid was extracted using the MagMax Pathogen RNA/DNA kit (ThermoFisher) per the manufacturer's instructions. Nucleic acid was extracted from between 100 μ L-1mL of the sample, depending on the sample type and microfluidic processing.

CMV total nucleic acid was quantified by qPCR using *Power SYBR*[®] Green RNA-to-*C_T*[™] (Applied Biosystems). Samples were assayed in triplicate with a total reaction volume of 10 μ L, including 3 μ L of a template and 0.3 μ L of each primer per the manufacturer's instructions. Thermocycling conditions were: 95 degrees for 10 minutes, followed by 45 cycles of 95 degrees for 15 seconds and 60 degrees for 60 seconds. Primer sequences were after Peres *et al.*⁵³: Forward=GAAGGTGCAGGTGCCCTG, Reverse=GTSTCGACGAACGACGTACG. Viral copies were calculated by comparison to a standard curve generated using a custom synthesized DNA fragment (gBlocks[®], IDT) quantified by NanoDrop (ThermoFisher Scientific). Final concentrations were adjusted for differences in sample volumes and dilutions during processing.

2.2.6 Viral next-generation sequencing (NGS)

Sequencing libraries were prepared from 1ng of extracted nucleic acid using the Nextera XT DNA library preparation kit (Illumina), as previously described⁴⁰. Sequencing libraries were quantified in triplicate using the KAPA Library Quantification kit (KAPA Biosystems) according to the manufacturer's instructions. Samples were pooled at equal molarity and sequenced on the Illumina MiSeq platform using paired-end 100bp reads.

Reads were demultiplexed, and an initial taxonomic assignment was performed using Kraken⁵⁴. Using viral-ngs⁵⁵, reads were cleaned of human reads, filtered against a reference genome corresponding to the HHV5 strain Merlin (NC_006273.2), and underwent *de novo* assembly of the CMV genome with refinement by scaffolding against the same reference genome. To compare CMV genome coverage between samples, 450,000 reads were randomly selected for each sample to ensure comparability, and then

CMV reads were aligned to the reference genome (NC_006273.2) in BWA using the following parameters -k 12 -B 2 -O 3; duplicate reads were excluded.

2.3 Results and Discussion

2.3.1 Evaluation of Spiral Microfluidic Device Performance

Particles or cells of different sizes experience different magnitudes of inertial and drag forces in a spiral microchannel and equilibrate at different lateral positions. Since the net lift force on a particle suspended in a plane Poiseuille flow is proportional to particle diameter (a_p) to the power of 4 ($\sim a_p^4$) ($F_L = \rho G^2 C_L a_p^4$, where ρ is the density of the fluid medium, G is the shear rate of the fluid given by $G = U_{max}/D_h$, U_{max} is the maximum fluid velocity, D_h is the microchannel hydraulic diameter, and C_L is the lift coefficient which is a function of the particle position across the channel cross-section and channel Reynolds number (Re)) and the Dean drag force on a particle is proportional to particle diameter ($\sim a_p$) ($F_D = 3\pi\mu U_{dean} a_p = 5.4 \times 10^{-4} \pi \mu De^{1.63} a_p$, where De (Dean number) is given by $De = \frac{\rho U_f D_h}{\mu} \sqrt{\frac{D_h}{2R}}$. U_f is the average velocity of the fluid, μ is the dynamic viscosity of the fluid, and R is the radius of curvature of the curved microchannel.)²³, larger particles or cells are more dominated by inertial lift force than Dean drag and tend to be equilibrated at the inner side of the spiral microchannel during operation. On the other hand, smaller particles are more dominated by Dean drag and tend to be dispersed throughout the microchannel, following two counter-rotating vortices known as Dean vortices in the spiral microchannel. Spiral microchannel is carefully designed to have a trapezoidal cross-section of 800 μm width, 70 and 40 μm height at inner-wall and outer-wall side, respectively, to focus relatively large host cells (RBC/WBC/Platelets, $\geq 3 \mu\text{m}$ in diameter) while relatively small virus particles are spread throughout the microchannel, as depicted in Fig. 4 A. Host cells are located near the inner-wall (IW) side of the microchannel when they reach the bifurcation point at the outlet and are fed back to the input tube during recirculation of spiral microfluidic device while virus particles are negatively selected and constantly collected at the outer-wall (OW) outlet. A trapezoidal cross-section was chosen to allow more space for the inner-wall focused host cells⁵¹ so

that the focusing behavior is maintained until the end of closed-loop operation when the concentration of the solution becomes higher. The inertially focused streamline of host cells at the inner-wall is further assisted by the Zweifach-Fung effect^{56,57} due to the smaller fluidic resistance. Thus the flow rate is higher at the inner-wall outlet. As can be seen in Fig. 4 C and D, the fluid collected at the OW outlet looked clear due to the depletion of host cells. This process takes place in an automated and fully contained manner, which can be compatible with biosafety requirements for processing known or unknown viral pathogens from clinical samples.

To evaluate the separation efficiency, we processed both whole blood and plasma samples. Figure 6 A illustrates the separation efficiency of our spiral microfluidic device operated in a closed-loop manner. For whole blood samples (n=9), the total number of RBC and WBC was reduced by 98% (from 6.7×10^8 to 1.5×10^7 cells), and the number of platelets was reduced by 36% (from 2.6×10^7 to 1.7×10^7 cells). For plasma samples (n=9), which should not contain RBC or WBCs but do contain residual platelets, the total number of platelets was reduced by 69% (from 2.4×10^8 to 7.4×10^7 cells). Depletion of platelets in the whole blood samples was found to be less effective than in the plasma samples because steric particle crowding effects became more severe for the whole blood samples and affected particle focusing behavior towards the end of C-sep when host cell concentration was highly increased.²⁴ The recovery of CMV nucleic acid was measured by qPCR from samples before and after microfluidic processing (Fig. 6 B). These results demonstrate the successful recovery of CMV from both whole blood and plasma across a range of viral concentrations. Overall recovery was calculated from the slope of data points and estimated to be 114.1% for whole blood samples and 103.5% for plasma samples. Estimated recovery greater than 100% could have come from sampling error or the inexact nature of qPCR.

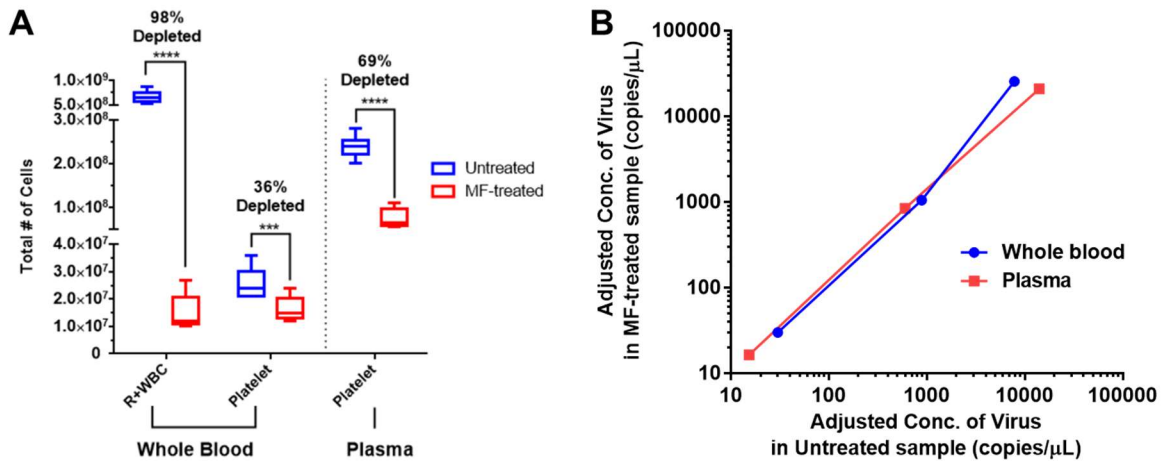


Figure 24 (A) Total number of cells (calculated from flow cytometry results) in untreated and MF-treated samples for whole blood and plasma samples. Each bar is drawn with data points of 9 samples. (B) Concentration of CMV (viral copies/uL) recovered as output from MF (y-axis) versus input (x-axis).

2.3.2 Assessment of virus genome recovery by metagenomic sequencing

We initially performed metagenomic sequencing from whole blood, plasma, and lysed plasma from a sample with a high viral load (10^8 CMV copies/mL of whole blood) before and after microfluidic separation. The lysed plasma sample was used as a control in which host cells and viruses are lysed prior to microfluidic separation; we expected that host nucleic acid would not be depleted by inertial microfluidics. To assess recovery of sequencing reads from CMV compared to host, we first performed metagenomic classification of all reads using Kraken.⁵⁴ This showed an increase in CMV reads and a decrease in human reads for both whole blood and plasma but not lysed plasma (Fig. 7 A). CMV reads increased from 2.0% to 4.0% for the microfluidics-treated whole blood sample and from 9.0% to 17.0% for the microfluidics-treated plasma sample, while CMV reads decreased from 2.0% to 0.8% for the microfluidics-treated lysed plasma sample, which may reflect sampling variability. Reads that were not classified as CMV or human belonged to microbial species that we commonly observe in our sequencing negative controls, representing background from water or sequencing reagents. We also assembled full CMV genomes and found an increase in the depth of coverage of the CMV genome by approximately 2 fold after microfluidic processing of both whole blood and plasma, normalizing for differences in total sequencing depth (Fig. 7 B). Depth increased for MF-

treated samples by 2.1 fold for whole blood (from 12 to 25) and by 1.8 fold for plasma (from 75 to 133), while coverage depth did not increase for lysed plasma samples.

The utility of spiral microfluidics for viral sequence enrichment was even greater at lower, clinically relevant viral loads (10^4 and 10^6 CMV copies/mL whole blood), levels at which full CMV genomes could not be assembled with the depth of sequencing used for the present study. To compare the recovery of CMV reads before and after microfluidic processing, we aligned all reads to the CMV reference genome and calculated the number of unique mapped CMV reads per sample. We observed a consistent increase in CMV reads after microfluidics, which was more pronounced in the whole blood than the plasma and at lower viral loads. Specifically, mapped viral reads increased after microfluidic processing by 16.5, 3.3, and 2.1 fold for whole blood samples and by 6.3, 2.0, and 1.9 fold for plasma samples with 10^4 , 10^6 , and 10^8 CMV copies/mL, respectively (Fig. 7 C and D). Furthermore, this increase in the number of CMV reads was evenly distributed across the full length of the CMV genome for both plasma and whole blood (Fig. 7 E). We do not observe evidence of a greater increase in the read depth for certain regions of the CMV genome (Fig. 7 E), indicating that microfluidics processing does not introduce biases in viral recovery. Overall, these results suggest that our spiral microfluidic platform enhances viral detection, especially in samples where the host background is higher and/or the viral content is low, as is the case for many clinical samples.

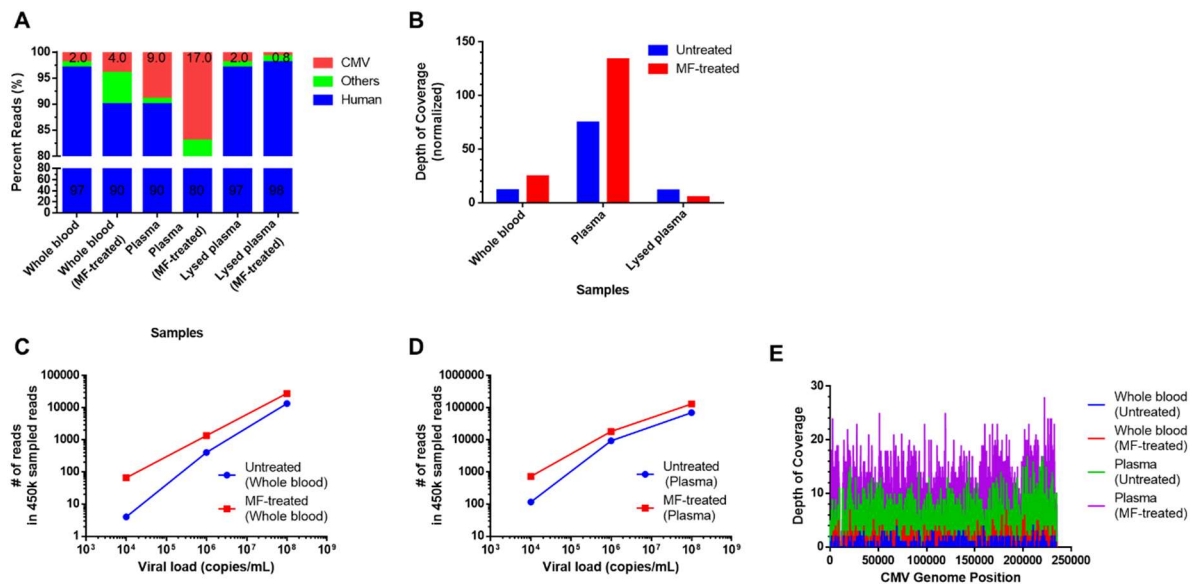


Figure 25 (A) Metagenomic classification of sequencing reads by Kraken for samples derived from whole blood spiked with 10^8 CMV copies/mL. (B) Normalized coverage depth of CMV whole-genome assemblies for samples in (A). (C) Comparison of CMV reads before (untreated), and after (MF-treated) microfluidic treatment of whole blood samples spiked with a range of CMV viral loads (10^4 , 10^6 , 10^8 copies/mL whole blood). (D) Comparison of CMV reads before (untreated) and after (MF-treated) microfluidic treatment of plasma samples (E) Plot showing the depth of coverage (y-axis) across the CMV genome (x-axis) in samples derived from whole blood spiked with 10^6 CMV copies/mL. Depth of coverage is the number of sequenced reads aligned to the CMV genome at each base pair position from 450,000 sampled reads.

2.4 Chapter conclusion

We developed a sample preparation platform using a spiral microfluidic device that can isolate viruses from host cells in whole blood or plasma in an automated, fully contained manner. Removal of host cells through size-based spiral inertial microfluidic sorting with recirculation led to the reduction of human (host) background reads in metagenomic sequencing for viral detection and sequencing. Further studies are needed to assess the recovery of intact infectious viruses for other downstream processes. We anticipate that our device can help ease the sample preparation process and improve the sensitivity of sequencing-based viral detection for viral clinical samples by enabling direct use of whole blood samples for WGS sample preparation as well as eliminating the need for a centrifuge or membrane-based filters.

Chapter 3

Clinical human blood sample lysis techniques

3.1 Motivation and background

It has been known that there exist only a few bacteria (~1-10 CFU/mL) in the blood samples of patients with clinically significant bacteremia that are recoverable via CFU plating.^{58,59} In order to recover and detect this very minimal amount of bacteria present in the bacteremic blood samples, many researchers and clinicians have adopted different approaches. As one of the most well-known methods, currently being the reference standard, culturing blood samples in liquid media has been adopted for decades because it can grow viable bacteria present in the samples and increase the number of bacteria by numbers of magnitudes so that they can be detected easily.⁶⁰ However, even for this gold standard method, it has its own shortcomings such as the long time required for culture and the inability to multiply microorganisms that are uncultivable.⁶¹ In an attempt to remedy this kind of issue, there has been a movement towards molecular diagnosis methods for bacteria detection directly from whole blood.⁶²⁻⁷¹ Molecular diagnosis methods, as known as PCR-based, has advantages such as reduced time to results and low detection limit due to its high sensitivity. However, their performance is often limited by the presence of vast human host DNA interfering with primers and probes used for PCR, so that blood samples need to go through certain processes to remove human DNA, for example, removal of white blood cells or degradation of human DNA. Moreover, PCR-based diagnosis is vulnerable to contaminants which may be introduced during sample collection or handling and result in false negatives.⁶¹

In order to circumvent these problematic issues of blood culture and PCR-based diagnosis, my research group has collaborated with Deborah Hung lab at Broad Institute, and Nanostring, a company that developed nCounter® platform that can provide molecular detection of target nucleic acids or proteins^{23,72} to find a solution that can identify bacteria in clinical bacteremic samples without culture or molecular amplification. Here, I would like to summarize the findings that I discovered from processing clinical bacteremic samples in the following sections. Bacteremic blood samples were kindly provided by Brigham and Women's Hospital, under an Institutional Review Board (IRB)-approved sample collection protocol.

At first, we tried to enumerate how many viable bacteria are present in bacteremic samples by plating the samples aliquoted and stored separately before blood culture and whose culture in liquid media later turned positive. These samples were classified as “old” blood samples because they were stored at 4°C for ~2-3 days before we got our hands on these samples. Interestingly enough, most of these “old” samples did not result in any CFUs when we diluted them 5 times in phosphate-buffered saline (PBS) or Luria-Bertani (LB) broth, plated and cultured them on LB agar plates (~0.5-1 mL of the original undiluted sample), even though they were the aliquots of the samples that turned positive in blood culture. From some literature search, it was found out that coagulation of blood induced by the intrusion of bacteria into the bloodstream enables entrapment of bacteria in blood clots and leads to immobilization and killing of these pathogens.⁷³⁻⁷⁵ Therefore, a number of blood lysis methods on these samples were tried to recover bacteria that are presumably entrapped in the blood clot (Figure 8), and we began to observe more samples that resulted in CFUs on the agar plates. After we started lysing the blood, we were able to recover viable bacteria on the LB agar plate for 79 out of 112 “old” samples (70.5% chance of finding viable bacteria). In the later phase of the project, we were able to access blood samples that were freshly drawn from patients within 24-48 hours of broad-spectrum antibiotics stewardship (classified as “fresh” blood samples hereafter). These patients' blood samples that were collected prior to antimicrobial stewardship turned positive in blood culture, and it was considered highly likely to have viable remnant bacteria in their freshly drawn blood sample. Although the chance of finding viable bacteria in these “fresh” samples was lower (12 out of 20 “fresh” samples, 60% chance) than the “old” samples, presumably due to blood

collection right after antimicrobial stewardship, we were still able to recover viable bacteria from the “fresh” samples with the blood lysis techniques applied.

In this chapter, I would like to introduce several blood lysis methods that can be adopted for clinical bacteremic blood samples to recover viable bacteria and compare the efficacy of each technique in the following sections.

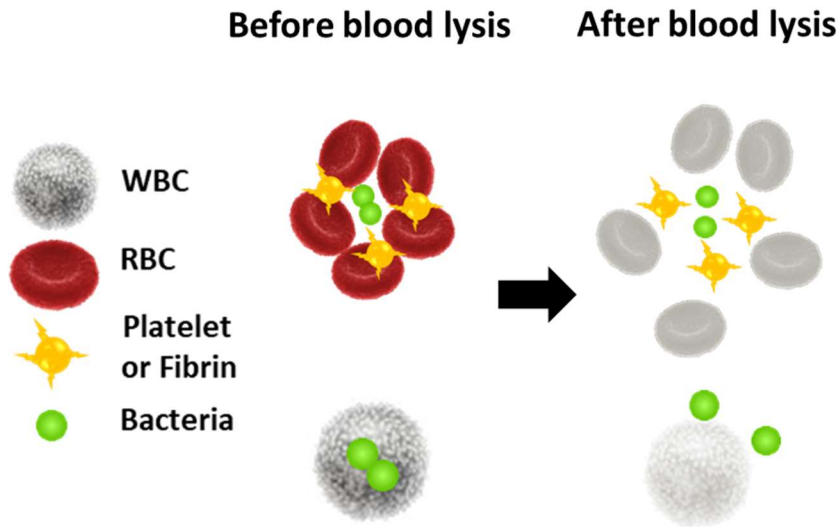


Figure 26 Schematic of bacteria entrapment in blood clot and discharge of them by blood lysis

3.2 Method

3.2.1 Deionized water-based blood lysis

There were two types of deionized water (DIW)-based blood lysis tried. The first type of DIW-based blood lysis included sample dilution with an isotonic solution and centrifugation step before DIW addition to the sample to induce greater hypotonic shock by DIW by removing the plasma part of the sample. Nine times the volume of phosphate-buffered saline (1x PBS) compared to the original blood sample is added, mixed with a blood sample, and centrifuged at 3,000 RCF for 15 minutes. The supernatant is carefully discarded using a serological pipette. Ten times to twenty times volume of DIW is added to the pelleted sample and vortexed gently for 30 seconds to perform hypotonic blood cell

lysis on the sample. It was found out that direct addition of DIW to the sample (9:1=DIW:blood, volume ratio) was enough to induce hypotonic lysis of blood cells, and the sample dilution with PBS and centrifugation step was skipped.

3.2.2 Red blood cell lysis buffer-based blood lysis

Red blood cell (RBC) lysis buffer (eBioscience, catalog no. 00-4333-57) was tried on a number of blood samples to lyse erythrocytes without inducing osmotic shock. RBC lysis buffer contains ammonium chloride, which is known to lyse RBC selectively with minimal effect on leukocytes. Ten times the volume of RBC lysis buffer is added to the blood sample and incubated at room temperature for 10 minutes until the solution becomes transparent red.

3.2.3 Saponin-based blood lysis

Saponin is a type of non-ionic surfactant that can be used as a blood cell lysis agent as it lyses red blood cells (RBC) by creating holes in the membrane and releases hemoglobin into the buffer.⁷⁶ Although DIW- or RBC lysis buffer-based blood lysis methods work fairly well, they both inevitably lead to volume increase up to ~10-20 times, which is not ideal for large volume sample processing (e.g. a few milliliters to tens of milliliters of blood). To resolve the issue of inevitable sample dilution, a high concentration of saponin stock solution (5% w.t.) is made by dissolving saponin in DIW or 1x PBS, and added to the blood samples, resulting in final saponin concentration of ~0.1-2.5% (w.t.).

3.2.4 Detoxification of saponin

In a patent filed by Wadley Research Institute and Blood Bank⁷⁷, saponin molecules with apparent molecular weight less than 600 are known to be toxic to microbial organisms. Detoxification of saponin refers to the process that can remove these toxic constituents through membrane filtration so that saponin can function as an effective hemolytic but is

not toxic to microorganisms. High concentration stock of saponin (10% w.t.) was prepared by dissolving saponin into DIW. This saponin solution was then loaded on centrifugal membrane filtration tubes (Spin-X UF 20 Concentrators with molecular weight cut-off of 5 kDa, Corning Inc., Corning, NY) and centrifuged at 3,000 RCF for 1 hour. Concentrate that remained on the membrane was collected, and DIW was added to the concentrate to compensate for the volume lost in the filtrate to constitute a stock solution of “detoxified” saponin (slightly less than 10% w.t.).

3.3 Results and discussion

3.3.1 Presence of bacteria in blood clots

At the beginning of the project, we had no idea of where bacteria in the “old” blood samples would be. These “old” samples were the samples that were stored separately at 4°C and whose culture turned positive in the liquid media culture later so that we had more confidence that they contained some viable bacteria inside. After plating both unlysed (diluted 5x in LB media) and lysed (DIW-based blood lysis, 1st type) samples of BLD_023, we observed that there were much more viable bacteria in lysed blood than unlysed blood (from Table 1, 82 vs. 4 CFU per mL of blood processed). We continuously observed this trend of having more bacteria in the lysed sample than the unlysed one for 14 more samples (Table 1). This suggests most of the viable bacteria in the “old” blood samples were trapped in the blood clot either by self-immunity of blood cells or due to the storage condition (sedimentation and coagulation), and we should lyse the blood samples from the beginning to recover most bacteria before we process and prepare these samples for further assays.

Table 4. Comparison of bacteria quantity between unlysed and lysed blood samples

Sample ID	Species	Bacteria in unlysed sample (CFU/mL)	Bacteria in lysed sample (CFU/mL)
BLD_023	Staphylococcus aureus	4	82
BLD_030	Staphylococcus aureus	58	315
BLD_051	Beta hemolytic Streptococcus group B	7	16
BLD_053	Escherichia coli	0	27
BLD_058	Klebsiella pneumoniae	20	89
BLD_060	Staphylococcus aureus	0	160
BLD_061	Staphylococcus aureus	0	234
BLD_063	Staphylococcus aureus	1	73
BLD_064	Streptococcus gordonii	0	207
BLD_067	Klebsiella pneumoniae	0	186
BLD_068	Staphylococcus aureus	0	103
BLD_069	Streptococcus thermophilus	0	160
BLD_070	Escherichia coli	1	61
BLD_071	Porphorymonas species, Coagulase negative Staphylococcus	0	12
BLD_072	Escherichia coli	0	14

3.3.2 Incomplete recovery of bacteria in blood clots by RBC lysis buffer

Three consecutive blood samples drawn from a single patient were used to compare the recovery of viable bacteria from blood samples lysed either by RBC lysis buffer or DIW (2nd type, direct addition of DIW to sample). As shown in Table 2, the number of viable bacteria per milliliter of blood is much higher in DIW-lysed samples than RBC lysis buffer-lysed samples. It suggests that DIW-induced hypotonic lysis of blood cells is more effective to recover bacteria from clinical bacteremic blood samples that might be trapped in blood clots than the RBC blood lysis buffer-based method. (Sample history: Sample ‘BLD_116’ and ‘BLD_117’ were “old” blood samples collected on February 2nd and 3rd of the year 2019, respectively, and shipped on February 5th, 2019. Sample ‘E-46 D0’ was a “fresh” blood sample, freshly drawn within 24-48 hours after antimicrobial stewardship, and it was collected and shipped on February 5th, 2019. All these samples

were confirmed to be infected with methicillin-susceptible *Staphylococcus aureus* (MSSA) by blood culture test.)

Table 5. Comparison of viable bacteria recovery from samples lysed by RBC lysis buffer and DIW

Sample ID	Species	Bacteria in RBC lysis buffer-lysed sample (CFU/mL)	Bacteria in DIW-lysed sample (CFU/mL)
BLD_116	<i>Staphylococcus aureus</i> MSSA	234	1570
BLD_117	<i>Staphylococcus aureus</i> MSSA	21	540
E-46 D0	<i>Staphylococcus aureus</i> MSSA	2	22

3.3.3 Effect of detoxification of saponin

For seven clinical bacteremic blood samples (one “fresh” blood sample and six “old” blood samples, all of which confirmed to be infected with MSSA) collected between April 30th and May 14th, 2019, three blood lysis methods (DIW, saponin, detoxified saponin) were applied to equal aliquots of each sample to see if there was a distinct difference between these methods. As shown in Table 3, the number of viable bacteria per milliliter of blood is quite comparable between DIW-lysed and detoxified saponin-lysed samples, but it is much lower in saponin-lysed blood samples. This implies that saponin-based blood lysis resulted in the poor recovery of bacteria in clinical bacteremic samples because of toxic components of saponin solution prior to detoxification. In other words, this result shows that toxic components of saponin were successfully filtered out by centrifugal filtration-based detoxification method, and the detoxified saponin is as effective as DIW to recover viable bacteria from clinical blood samples.

Table 6 Comparison of viable bacteria recovery after applying three different blood lysis methods (DIW, saponin, detoxified saponin)

Sample ID	Species	Bacteria in DIW-lysed sample (CFU/mL)	Bacteria in Saponin-lysed sample (CFU/mL)	Bacteria in Detox. Saponin-lysed sample (CFU/mL)
E-63 D0	<i>Staphylococcus aureus</i> MSSA	13	0	21
BLD_148	<i>Staphylococcus aureus</i> MSSA	224	51	128

BLD_149	Staphylococcus aureus MSSA	13	0	6
BLD_150	Staphylococcus aureus MSSA	5	0	7
BLD_151	Staphylococcus aureus MSSA	14	0	9
BLD_152	Staphylococcus aureus MSSA	977	379	919
BLD_154	Staphylococcus aureus MSSA	18	0	11

3.4 Chapter conclusion

We have shown that we can recover more viable bacteria in clinical bacteremic blood samples by lysing the blood than just using unlysed, whole blood. It is not entirely clear by what mechanism bacteria are trapped in the blood clots, but the results from plating the unlysed and lysed samples suggest that most of the viable bacteria in the clinical bacteremic blood samples were trapped in the blood clot and were released by the blood lysis. Moreover, we were able to demonstrate that some blood lysis methods such as the DIW-based hypotonic lysis or the use of detoxified saponin are more desirable and effective to recover bacteria in these clinical samples than other methods such as the use of RBC lysis buffer or unpurified saponin. We believe that our experience on the clinical bacteremic blood samples would be not only helpful for our own development of blood sample preparation protocol but also informative to other researchers and clinicians who are seeking to detect and recover viable bacteria from these samples.

Chapter 4

Rapid bacteria detection from blood samples without culture or PCR²

4.1 Motivation and background

Bloodstream infection (BSI) such as bacteremia or sepsis has been considered a major cause of mortality worldwide. In treating BSI, rapid detection of bloodborne bacteria is essential because BSI-related morbidity or mortality can be significantly reduced if we can identify pathogenic bacteria in the early stage of infection⁷⁸. Isolation and identification of bacteria from bacteremic blood are rendered difficult due to the extremely low abundance (~1-5 CFU/ml) of bacteria and the presence of large molecular and cellular backgrounds. Therefore, diagnosis of bacterial infection has been relying on blood culture methods or molecular amplification techniques such as polymerase chain reaction (PCR) to increase the number of bacteria cells or nucleic acids. However, these methods usually require a long time before diagnosis, induce bias or result in false positives because of their high sensitivity⁷⁹.

² The following published conference paper was used in its entirety for Chapter 3, with minor updates and modifications:

Choi, K.; Ouyang, W.; Ryu, H.; Han, J. "CULTURE- AND PCR-FREE DETECTION OF LOW ABUNDANCE BACTERIA FROM BLOOD WITHIN AN HOUR", *The 22nd International Conference on Miniaturized Systems for Chemistry and Life Sciences (MicroTAS)*, Nov. 11-15, 2018, Kaohsiung, Taiwan

Contributions: K.C., W.O. and J.H. conceived of the approach and designed the experiment. H.R. contributed to the operational scheme of the spiral microfluidic sorter. K.C. contributed to the design, fabrication, execution of experiment regarding the spiral microfluidic sorter device. W.O. contributed to the design, fabrication, and execution of experiment regarding the electrokinetic microfluidic concentrator device. K.C. and J.H. mainly drafted the manuscript, which all authors have read and reviewed.

Recently, a lot of effort has been made in microfluidics to enhance the sensitivity of nucleic acid (NA) detection in biological samples by capturing nucleic acids in the device and eluting them out for further downstream assays.^{80–83} However, most of these approaches remained in the realm of miniaturizing solid-phase extraction (SPE) in micro-chambers with high surface area silica⁸⁴ or other polymers such as poly(methyl methacrylate) (PMMA)⁸⁵, polycarbonate (PC)⁸⁶, packed silica beads⁸⁷ or magnetic beads functionalized with polythymine deoxyribonucleotides (oligo-dTs)⁸⁸, usually followed by elution and subsequent PCR. Our group, on the other hand, has been focusing on ion-concentration polarization (ICP)-based electrokinetic trapping (ET) method, which can not only capture and purify NAs in the microfluidic device but also detect them on the same platform without any chemical amplification of biomolecules using the electrical property of these biomolecules. It is known to be a method that can concentrate NAs in biological samples quite rapidly (~a few tens of minutes) while achieving high enrichment factors up to $\sim 10^6$.⁸⁹

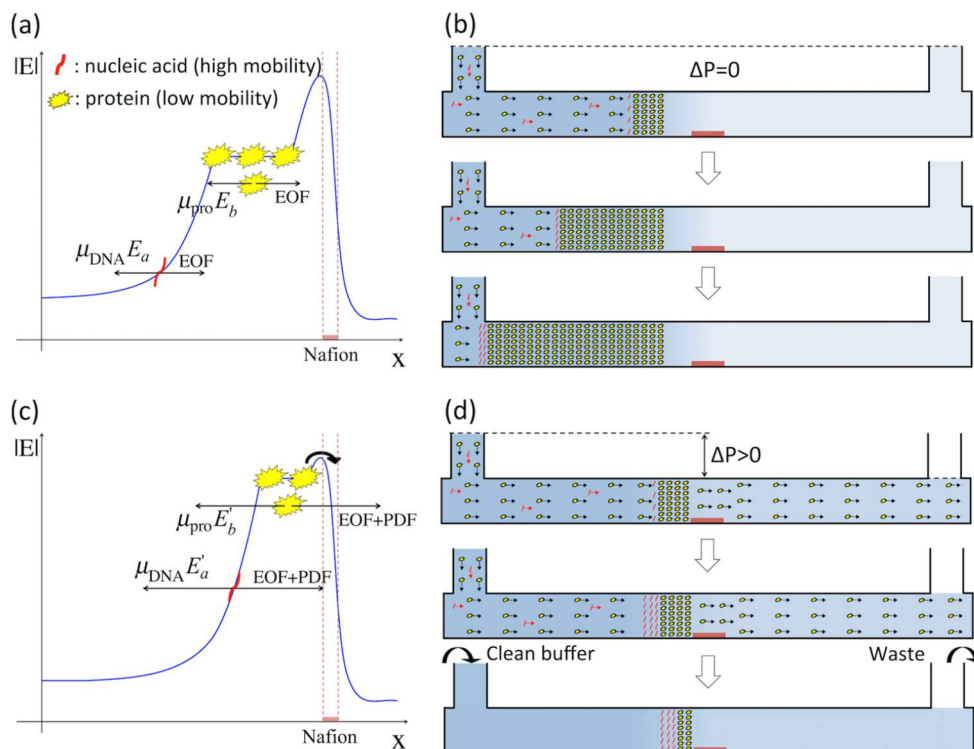


Figure 27 Schematic of pressure-modulated selective electrokinetic trapping (PM-SET) principle. (a, c) Concentration of nucleic acids and proteins at zero external hydrostatic pressure. Nucleic acids have higher electrophoretic mobility than proteins, locating farther from the Nafion membrane. (b, d)

Concentration of nucleic acids and proteins at existent external hydrostatic pressure. Proteins overcome the electrostatic barrier and leak through the membrane while nucleic acids are still electrokinetically trapped before the barrier, thus become concentrated and purified. Reprinted with permission from (Ouyang *et al.*, *Anal. Chem.* 2018, 90, 19, 11366-11375). Copyright (2018) American Chemical Society

In ICP-based ET concentrator devices, an ion-depletion zone is created in the micro-channel by a selective transport of cations through a cation-exchange membrane (CEM) under a direct-current (DC) electric field. Since the ion-depletion zone is devoid of electric charge, a significant portion of the DC electric field is applied at this zone due to the increased electric resistivity. It builds an electric barrier to negatively charged particles such as NAs and proteins so that they cannot pass through, accumulate before this zone, thus become concentrated (Figure 9). ICP-based ET is regarded as a promising method for concentrating biomolecules because it can continuously concentrate negatively charged biomolecules and is insensitive to electrically neutral contaminants, not to mention that it is reagent-free and can be easily integrated with downstream processes.⁸⁹⁻⁹¹

In this chapter, we aim to demonstrate the detection of bacterial species from approximately 1-5 CFU/ml blood samples by the combination of high throughput spiral microfluidics³ and ICP-based ET concentrator devices⁹². In order to enable this, we had to significantly improve the performance of both spiral sorter and concentrator by multiplexing (to increase throughput) and multi-staging (to enhance the performance). The process utilizes 8 spiral sorter devices running in parallel for two-stage blood separation, followed by 640 ICP-based ET concentrators running in parallel for two-stage preconcentration-hybridization (Figure 10), by which one can process and identify bacteria species from 1 mL blood sample within 1 hour, which is faster than any other studies reported, to our best knowledge. Moreover, our approach does not require amplification steps because our concentrator device can physically concentrate the rRNA-probe conjugates at the nanojunction, even at low abundance.

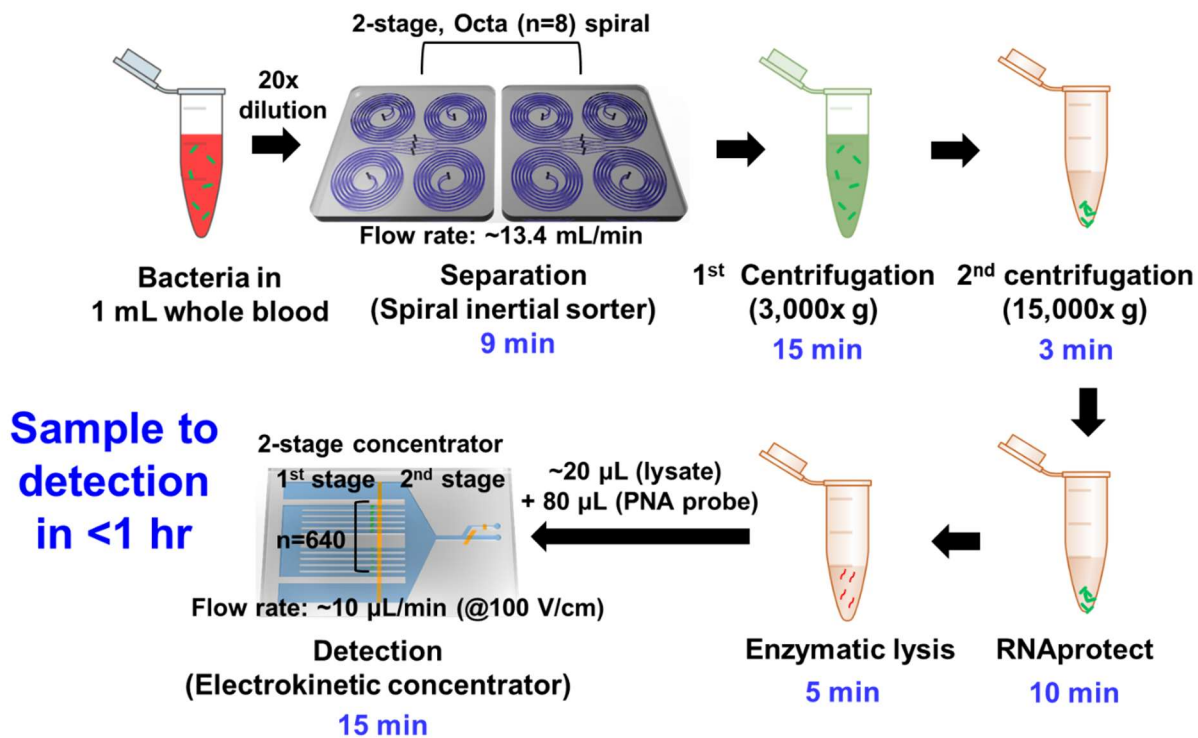


Figure 28 Overall flow chart of our platform for the separation and detection of bacteria from a blood sample

4.2 Method

4.2.1 Fabrication of microfluidic devices

Both spiral inertial sorter and electrokinetic concentrator devices were fabricated with polydimethylsiloxane (PDMS) following standard soft-lithographic microfabrication techniques described previously.^{3,92,93}

4.2.2 Preparation of bacteria-spiked blood samples

Green fluorescent protein-expressing *Escherichia coli* (GFP *E. coli*, ATCC® 25922GFP™, ATCC), *Pseudomonas aeruginosa* (*P. aeruginosa*, ATCC® 15442™, ATCC), and *Klebsiella pneumoniae* (*K. pneumoniae*, ATCC® BAA-1705™, ATCC) were cultured and plated as per ATCC's instruction. Bacteria was spiked directly into whole blood samples at a concentration of 1-1000 CFU/mL at the beginning of the experiment. The number of bacteria in each sample (unlysed) was enumerated using a CFU plating method to evaluate bacteria recovery after spiral cell sorting operation.

Bacteria load in each lysate sample that was loaded onto an electrokinetic concentrator was estimated by plating the same amount of bacteria stock that was spiked into the initial sample.

Multiple dilutions (5, 10, 20, and 100 times) of blood in phosphate-buffered saline (PBS) with 0.1% (w.t.) bovine serum albumin (BSA) and 2 mM Ethylenediaminetetraacetic acid (EDTA) were prepared and tested for spiral sorter through various flow rate range to determine minimum dilution required for blood cell separation using negative selection scheme (Figure 11).

4.2.3 Process workflow

The entire process workflow was executed as shown in Figure 10. For the 2-stage spiral sorter operation with negative selection, 20 times dilution of blood sample and 1.6 mL/min per spiral device was chosen as the operating condition as it was deemed optimal for separating blood cells with minimal dilution for shorter processing time while maintaining separation efficiency.

Consecutive centrifugations ($3,000\times g$ for 15 minutes and $15,000\times g$ for 3 minutes) were applied to spiral-processed samples to collect bacteria in a smaller volume. 50 μL of RNAprotect (Qiagen) was added to the collected bacteria, and the mixture was vortexed for 5 seconds, followed by incubation for 5 minutes at room temperature to stabilize RNA present in the sample. The bacteria sample was centrifuged again at $15,000\times g$ for 5 minutes to remove the remaining RNAprotect. The cell pellet collected after RNAprotect was lysed with 18 μL of 1 mg/mL lysozyme and 1 unit/ μL SUPERase[•]In (Invitrogen) inhibitor in $0.1\times$ PBS for 5 minutes to yield bacterial nucleic acids. The lysate was added with 1.8 μL of $10\times$ PBS to adjust the salinity, incubated with 80 μL of fluorescence-labeled PNA that is specifically designed to hybridize with 16s rRNA of *E. coli* and loaded onto the electrokinetic concentrator.

For electrokinetic concentrator operation, 200V was applied across the 1st stage microchannel of the electrokinetic concentrator for 10 minutes to transport as well as to concentrate the rRNA-probe at the 1st nanojunction. The same voltage was applied across

the 2nd stage microchannel for 5 minutes to concentrate the rRNA-probe at the 2nd nanojunction further.

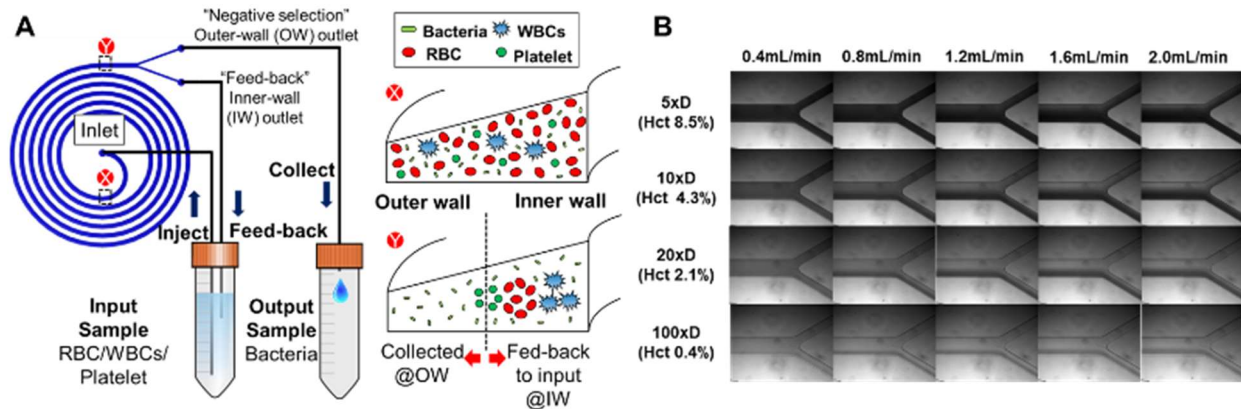


Figure 29 (A) Schematic of a spiral inertial microfluidic device with negative selection scheme for bacteria separation from blood (B) Microscope images of cell sorting behavior for different hematocrit and flow rates

4.3 Results and discussion

4.3.1 Evaluation of spiral cell sorter performance

Separation of bacteria from abundant host blood cells was done by a 2-stage spiral inertial microfluidic sorter. The two-stage spiral device with a negative selection scheme enabled high recovery of bacteria (>90%, down to ~3 CFU/mL level) while removing most of the host cells (>99% of RBC and WBCs and ~40% of platelets) in the blood samples by keeping the focused host cell streamlines to the internal feedback loop (Figure 12).

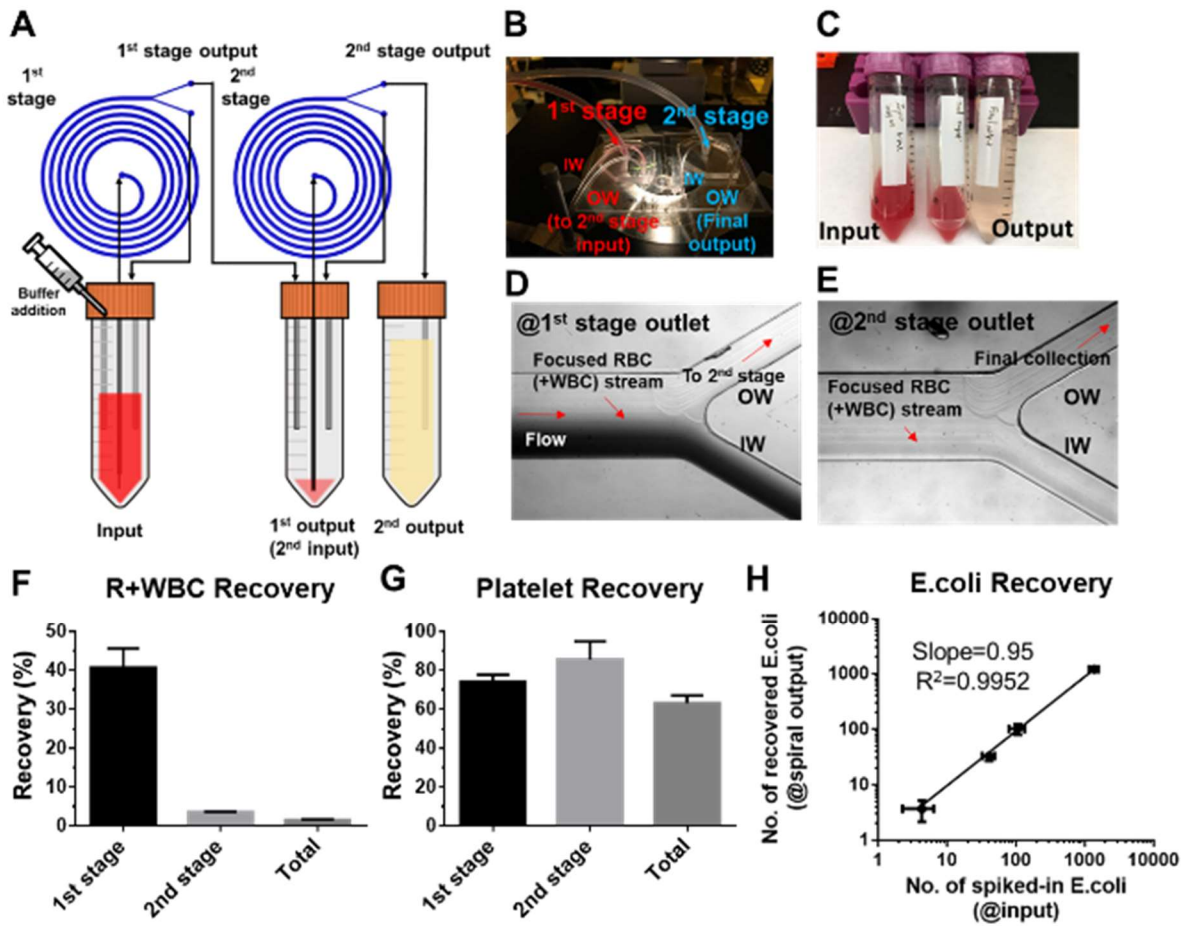


Figure 30 (A) Schematic of 2-stage spiral device operation (B) Photograph of actual device setting (C) Photograph of treated samples (D)-(E) Microscope images at inlet and outlets (F)-(G) Host cell sorting performance at each stage (H) Number of E.coli recovered at the spiral output (2nd stage) (y-axis) for multiple loads of bacteria at the input (x-axis)

4.3.2 Evaluation of electrokinetic concentrator performance

Spiral device-processed samples which contained most of the bacteria in a new buffer went through centrifugation and bacterial lysis to yield bacterial rRNA for specific species identification. The bacterial lysate was incubated with the fluorescence-labeled PNA probe (neutral in charge, unconcentratable in the electrokinetic concentrator) and the rRNA-probe conjugate was concentrated by over million-fold (confirmed by comparison of fluorescence intensity before and after concentration) within 15 min using the two-stage 640-plex ICP-based concentrator (Figure 13).

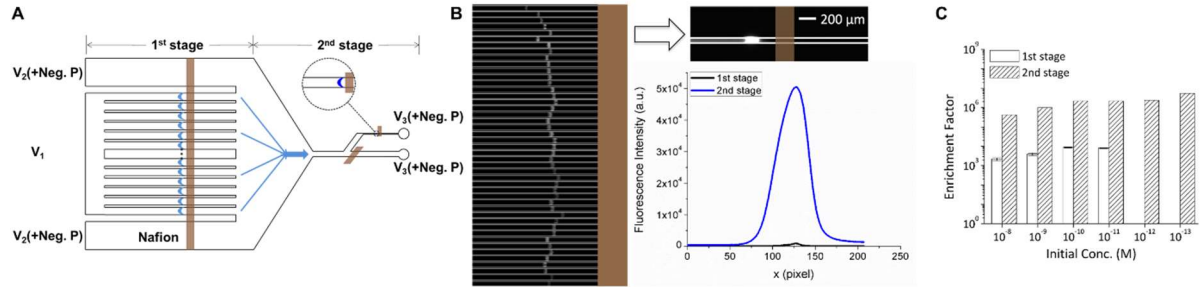


Figure 31 Schematic of the two-stage 640-plex electrokinetic concentrator. (A) Principle and design of the device. (B) Fluorescence images showing the concentration of fluorescent DNA in the first stage and second stage. The fluorescent intensity was significantly boosted by two-stage concentrating. (C) The concentration factor achieved by the 640-plex device. Over a million-fold was achieved within 15 min.

4.3.3 Evaluation of detection sensitivity and specificity

Detection of *E. coli* was verified with fluorescence microscopy to a level of ~ 1 bacteria load lysate, and the fluorescence intensity was shown to be linearly proportional to the number of bacteria spiked in (Figure 14). For the detection of ~ 1 bacteria lysate, a split of the lysate was used when the sample was found to have had more than 1 bacterium in it (*i.e.*, split the lysate into 3 for a sample known to contain ~ 3 *E. coli*). The specificity of the *E. coli* PNA probe binding was also verified by the low fluorescence intensity of other bacteria lysates containing ~ 1000 CFUs of *P. aeruginosa* and *K. pneumonia* when incubated with the probe.

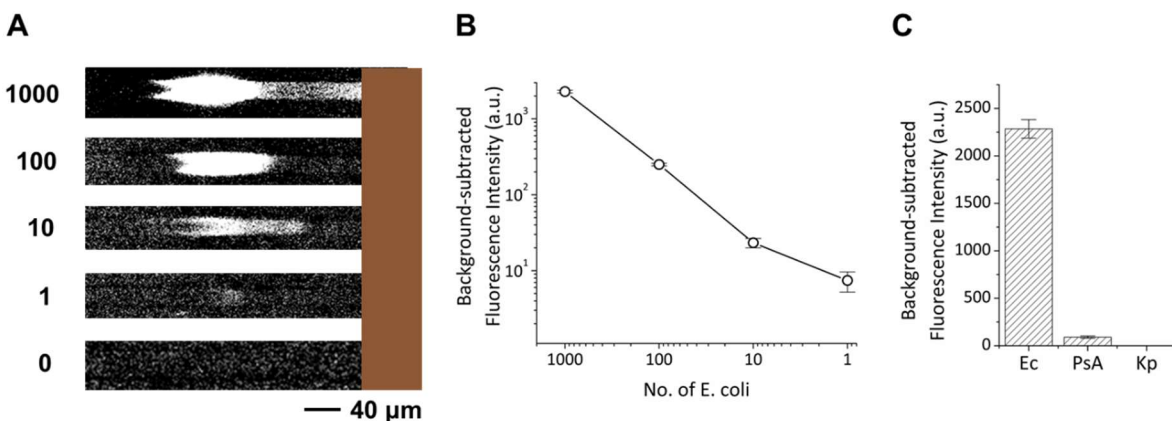


Figure 32 Bacteria detection using the two-stage concentrator. (A) Fluorescence images showing the PNA-rRNA complex at different numbers of *E. coli* cells. (B) The dependence of fluorescence intensity on the number of bacteria. ($n=3$) (C) Specificity of detection across bacteria species. ($n=3$)

4.4 Chapter Conclusion

We have demonstrated detection of low abundance bacteria from blood down to $\sim 1-5$ CFU/mL level by separating bacteria from blood cells with spiral microfluidics and concentrating rRNA-probe conjugate with an electrokinetic concentrator. The entire process only takes less than an hour because culture or PCR is not performed, which usually takes a longer time and might cause false positives or the introduction of amplification bias. We believe our entire workflow for bacteria separation and detection does not only enable rapid diagnosis of BSI but also open up a possibility of on-chip bacteria detection without requiring high-profile analyzers such as sequencer or mass spectrometers.

Chapter 5

Scalable and Continuous Cell Washing Method by Spiral Inertial Microfluidics for Adventitious Agent Clearance

5.1 Motivation and background

Recently, more and more effort has been put to develop technologies that can better accommodate continuous bioprocessing such as continuous cell washing⁹⁴⁻¹⁰⁰, in-line monitoring¹⁰¹⁻¹⁰³ and perfusion bioreactors¹⁰⁴⁻¹⁰⁷ for both large-scale production (*e.g.* large molecule drugs like monoclonal antibodies (mAbs) and vaccines) and small-scale production (*e.g.*, treatments for orphan diseases and personalized cell/gene therapies).

Cell washing/concentration is a necessary step in the biomanufacturing process, either to re-suspend cells in a specific medium that is appropriate for cells to replicate at upstream bioprocessing, or to clarify cells by removing impurities such as residual metabolites and adventitious agents (AAs) from the original sample at downstream bioprocessing.¹⁰⁸ For example, working cell banks (WCB) that are derived from master cell banks (MCB) and used for large-scale production need to be thawed and appropriately washed before cell expansion to remove residual metabolites and to replace the buffer with a fresh medium. Since WCBs do not go through intensive adventitious agents testings as MCBs¹⁰⁹, it is important that cell washing is performed in a carefully controlled, sterile environment by skilled personnel. Nowadays, cell therapy products such as chimeric antigen receptor T cell (CAR-T) require mitigation of the risk posed by AAs as it is directly related to patient safety. Also, these products cannot usually go through all necessary safety tests, including compendial sterility testing for AAs before product release due to the limited shelf life and production time.¹¹⁰ Conventional cell

washing/concentration is generally achieved by centrifugation to generate a packed cell pellet, followed by removing the supernatant and replenishing a new buffer solution. However, some of the cell washing steps that are manually conducted in an open environment can expose cells to external contamination.^{111,112} In addition, productivity or functionality of cells can be affected by shear stress from rigorous centrifugation and pipetting to break cell clumps, which also causes the issue of reliability and repeatability of the process.^{113–115} Such cell perturbations are not desirable, especially for live-cell products such as CAR-T, due to the limited number of cells produced and the unknown effects of such perturbations *in vivo*.

As an alternative to manual processes based on centrifugation, automated cell washing/concentration technologies based on membrane filtration such as alternating tangential flow filtration (ATF) or tangential flow filtration (TFF) are recently adopted by bio-manufacturers.^{116–118} Clogging is minimized by cross filtration where cells are retained in the flow direction along with the fluid inside the membrane while the filtrate passes through the membrane in the normal direction to the fluid during operation. However, large hold-up volume and frequent replacement of the membrane due to accumulated biofouling limit the scalability of the process and can impact cell viability and quality, respectively.¹¹⁹ Another technology called acoustic wave separation (AWS) has been proposed as a membrane-less filtration method to clarify harvested cell culture fluid (HCCF) and remove residuals from cell culture.^{120–122} In AWS, an acoustophoretic wave generates nodes in the flow channel where suspended cells are trapped, form aggregation, and settle down. Although this technology does not require a membrane, it has limited application only for cells that can form clusters, as non-aggregated cells cannot be recovered by this method. Moreover, prematurely induced aggregation of cells can lead to variability in mass transfer and cell signaling, heterogeneous differentiation of cells, thus potentially compromising the quality and yield of cellular product.¹²³ Gravity-driven sedimentation processes are also employed in an inclined settler system to induce sedimentation of cells for separation¹²⁴, but are generally limited by large hold-up volume due to weak gravitational forces and slow sedimentation speed. Other relatively new cell washing/concentration systems that are currently available for cell and gene products are mostly based on automation of centrifugation^{95–98} (*e.g.*, Miltenyi CliniMACS Prodigy, Corning X-wash, Gibco CTS Rotea, and Sepax) or a combination of two methods such as spinning membrane

where centrifugation and membrane filtration is combined⁹⁹ (e.g., Fresenius Kabi LOVO).

Recently, inertial microfluidics has attracted considerable attention due to its versatile and straightforward way of separating particles based on particle size in various sample volumes (mL to L) without necessitating any labeling or external driving force other than the pumping system.¹²⁵ In inertial microfluidics, particles of different sizes are separated in the microchannel because they undergo different magnitudes of hydrodynamic forces called net lift force and drag force.⁴⁶ Since the separation of particles is purely dependent on hydrodynamic forces applied to particles, an inertial microfluidics-based sorting system need not use a membrane. In addition, inertial microfluidic devices can be easily scaled up to process large volume samples with high throughput up to 1 L/min using multiple channels and layers in parallel.^{49,126,127} Due to such advantages, inertial microfluidics-based cell separation has been applied to various biological/physiological samples in different volume scales and demonstrated better outcomes such as less disturbance on cell functionality or higher purity of the final sample.^{4,21,22,128} For example, in the field of biomanufacturing, researchers have applied this sorting method as a membrane-less cell retention device.^{49,129} The fact that inertial microfluidics-based cell sorting can achieve fast and efficient separation of cells without disrupting cell functionality, productivity, and viability^{49,128,129} has enabled its use as a cell retention device for long-term perfusion culture of suspended mammalian cells.

In this chapter, we present a spiral inertial microfluidic system that can achieve automated, continuous, clog-free cell washing/concentration. The cell washing/concentration system is based on our previous sorting scheme called negative selection, where large cells form a focused streamline and are retained in a closed feedback loop. At the same time, small particles like viruses are continuously collected at the non-cell-focusing side of the microchannel.³ With this scheme, adventitious agents such as bacteria and viruses that are usually small compared to the cells of interest (e.g., Chinese hamster ovary (CHO) cells or T cells) can be continuously washed away from the focused, retained cells of interest. We also devised a scheme called “constant medium addition” to achieve further cell washing in the system (Fig. 15). Fresh and sterile medium is constantly replenished to the input reservoir at the same volumetric rate of the outer-wall outlet sample (waste) collection. The cell washing can be continued until the desired level of adventitious agent clearance is achieved. We verified the efficacy of cell washing by

comparing the concentration of contaminants in the input before and after washing via fluorescence microscopy, colony-forming unit counting, and quantitative real-time PCR (qPCR). It was shown that our spiral microfluidic sorter could effectively wash away free-floating, non-adherent adventitious agents up to LRV of 4.32 and 2.03 for bacteria and virus, respectively, with ten to fifteen times the volume of washing medium with respect to the original sample used. We envision that our membrane-less, scalable, continuous cell washing/concentration technology can offer many advantages over currently available ones such as ATF, TFF, or AWS and can be applied to a wide range of bioprocesses ranging from downstream cell washing for cell therapy products to large-scale upstream cell clarification.

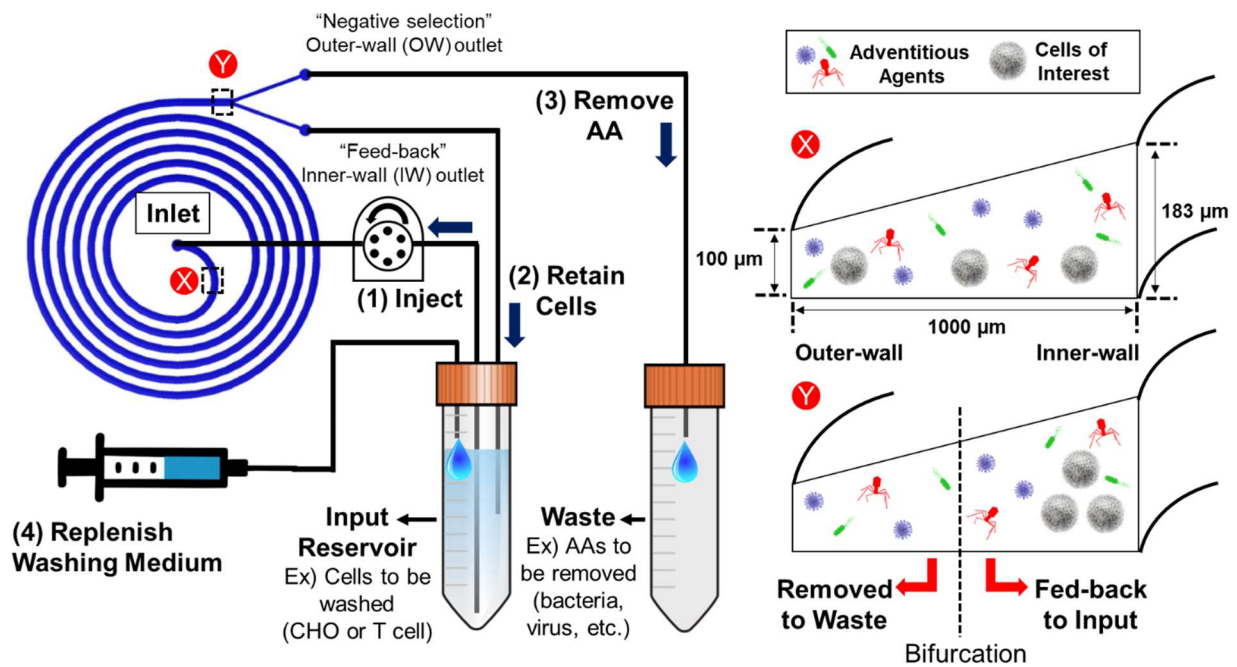


Figure 33 Constant medium addition scheme of spiral microfluidic sorter operation for cell washing. The sample is drawn from the input reservoir and injected into the spiral sorter using a peristaltic pump at the inlet. Two streams of outputs are generated at the outlet bifurcation: 1) inner-wall (IW) outlet stream where most of the cells that are focused near the inner-wall of the microchannel are flowing and 2) outer-wall (OW) outlet stream where the fluid contains mostly free-floating adventitious agents. Adventitious agents are constantly removed towards the waste stream (OW outlet) with continuous addition of a medium while cells of interest (e.g., CHO cells, T-cells) are retained at the IW outlet and fed back to the input reservoir. Media is continuously added to maintain the cell density at the input reservoir and to wash out adventitious agents towards the waste stream.

5.2 Method

5.2.1 Fabrication of spiral microfluidic cell sorter

A Spiral inertial microfluidic sorter was fabricated with polydimethylsiloxane (PDMS) in accordance with standard soft-lithographic microfabrication techniques.³ The aluminum master mold was fabricated with a micro-milling machine (Whits Technologies, Singapore). The mold design was drawn with AutoCAD software. Sylgard 184 PDMS base and curing agent (Dow corning Inc.) were mixed with a 10:1 mass ratio and degassed in a vacuum desiccator for 30 minutes. The degassed mixture was cast on the aluminum master mold and cured on a hot plate for 10 minutes at 150 degrees. A cured replica was peeled off from the mold after it was cooled down to room temperature. Inlets and outlets of the device were punctured using disposable biopsy punches (Integra™ Miltex®) for tube connection for fluidic transport. The cured PDMS replica with punctured holes was then permanently bonded to a glass slide after treating both the PDMS surface and the glass slide with a plasma machine (Femto Science, Korea) at 100W for 45 seconds (ambient air at 0.5 Torr or 66.7 Pa). The fabricated spiral microchannel was measured to have a trapezoidal cross-section and had dimensions of 183 μm height at the inner-wall, 100 μm height at the outer-wall, and 1000 μm width.

5.2.2 Preparation of CHO cell culture

CHO cells (FreeStyle™ CHO-S Cells, Thermo Fisher Scientific) were grown in a 5% CO₂ incubator (Forma Steri-Cycle 370, Thermo Fisher Scientific) at 37 degrees, contained in a glass spinner flask (4500-500, Corning) spun at 65 RPM. Cells were seeded at 0.3 million cells/mL cell density into a pre-warmed (37 degrees) culture medium (FreeStyle™ CHO Expression Medium, Thermo Fisher Scientific) to have a total culture volume of 200-250 mL. Cell culture parameters such as cell density, viability, average cell diameter, nutrient and metabolite concentrations, ion

concentrations, and pH were analyzed by an automated cell culture analyzer (BioProfile® FLEX2, NovaBiomedical) and were monitored regularly throughout the culture.

5.2.3 Preparation of fluorescent beads, bacteria, and virus-spiked samples and characterization of clearance

CHO cell culture at 1-3 million cells/mL with high viability (>95%) was used for the adventitious agent clearance experiment. For evaluation of plastic beads clearance, fluorescent polystyrene beads (Fluoresbrite® YG Microspheres 1.00µm, Polysciences, Inc.) were spiked into a CHO cell culture sample at a concentration of 40-100 million beads/mL initially. Aliquots of samples collected at different time points of cell washing were analyzed by fluorescence microscopy using a hemacytometer (C-Chip™ Disposable Hemacytometers, INCYTO, Korea). For evaluation of bacteria clearance, green fluorescent protein-expressing *Escherichia coli* (ATCC® 25922GFP™, ATCC) was spiked into CHO cell culture sample at a concentration of 100-300 million CFU/mL at the beginning of the experiment, and aliquots of samples collected at later time points of cell washing were analyzed by fluorescence microscopy using a hemacytometer and CFU plating method. GFP *E.coli* was cultured and plated as per ATCC's instruction (Tryptic Soy Agar/Broth with 100 mcg/mL Ampicillin at 37 degrees in aerobic condition). For evaluation of virus clearance test, minute virus of mice (MVM, Rodent protoparvovirus 1 (ATCC® VR-1346™)) was spiked into CHO cell culture sample at a concentration of 20-200 million viral copies/mL at the start. Samples at different washing time points were collected and extracted with a nucleic acid extraction kit (PrepSEQ™ 1-2-3 Nucleic Acid Extraction Kit, Thermo Fisher Scientific) as per the manufacturer's instructions. MVM viral DNA was quantified with quantitative real-time PCR using a commercial MVM detection kit (ViralSEQ™ Mouse Minute Virus (MMV) Detection System, Thermo Fisher Scientific) and an analyzer (LightCycler® 480 System, Roche Life Science, Germany). Extracted samples were analyzed in triplicates to a total reaction volume of 30 µL including 10 µL template, 15 µL of 2× Environmental Master Mix, 3 µL of 10× MVM Assay Mix and 2 µL DI water. The thermal cycling condition for qPCR was 95

degrees for 10 minutes, followed by 45 cycles of 95 degrees for 15 seconds and 60 degrees for 60 seconds. Viral copy number was calculated by generating a standard curve using a positive control from the MVM detection kit with known viral DNA copy number (1000 copies/ μ L) and serially diluted stocks of MVM.

5.2.4 Continuous cell washing by constant medium addition

Spiral inertial microfluidic sorter was operated at 4 ml/min input flow rate in a closed-loop mode of separation (“C-sep”) ^{4,129} where the cell-focused side of the bifurcated outlet channel is fed back to the input reservoir so that cells of interest are retained while adventitious agents-containing, the non-cell-focused portion is negatively selected and removed to a waste stream (Fig. 15). Continuous cell washing was realized by constantly adding a sterile medium to the input reservoir at the volumetric rate that matches the waste collection rate. The addition of the medium serves two purposes: 1) to keep the cell density at the input reservoir so that cell separation efficiency is maintained during the entire operation with constant width of the cell-focused streamline; 2) to enable continuous washing until the desired level of purity or LRV is achieved.

A peristaltic pump (Masterflex® L/S® Standard Digital Pump Systems, Cole-Parmer) and compatible tubing (Masterflex platinum-cured tubing, L/S 14, Cole-Parmer) were used to configure the closed-loop mode of operation, connecting the device to a pump and transporting the samples from each bifurcated outlet to corresponding sample tube (Falcon® Polystyrene Sterile Centrifuge Tubes, Corning®). A syringe pump (PHD 2000, Harvard Apparatus), plastic syringe (BD Luer-Lok tip syringe, Becton Dickinson), and the same tubing were used to construct a constant medium addition module (Fig. 15).

5.2.5 Neuraminidase treatment

Sialic acid is known to be used as a receptor for cell entry by many viruses.¹³⁰ As an attachment to a receptor on a cell membrane is an imperative step for a virus to enter and

infect the cell. Several researchers have developed a CHO cell line that is resistant to MVM by genetically engineering a CHO cell to express no sialic acid on the cell membrane.¹³¹ Inspired by this, we have adopted the use of neuraminidase (sialidase) to remove sialic acids on the CHO cell membrane so that attachment of MVM to the CHO cell membrane can be minimized and the efficacy of cell washing can be maximized.

Neuraminidase (from *Arthrobacter ureafaciens*, Roche, Switzerland) was added into CHO cell culture samples to a concentration range of 20-100 mU/mL. Neuraminidase-added samples were incubated at 37 degrees for an hour in an orbital shaker rotating at 120 RPM before the virus spike-in.

5.2.6 Evaluation of spiral microfluidic cell sorter performance

The cell separation efficiency of a spiral microfluidic cell sorter was evaluated using cell recovery, which is expressed as the following equation:

$$\text{Cell recovery (\%)} = \frac{(\text{total number of viable cells in the washed sample})}{(\text{total number of viable cells in the initial sample})}$$

where the total number of viable cells is calculated by multiplying the viable cell concentration of a sample measured by BioProfile® FLEX2 analyzer and the volume of a sample.

Log reduction value (LRV) was used as a measure of adventitious agent clearance, which is expressed as follows:

$$\text{LRV} = -\log_{10}\left(\frac{\text{concentration of adventitious agent in the washed sample}}{\text{concentration of adventitious agent in the initial sample}}\right)$$

where concentration of adventitious agent is quantified by hemacytometer or CFU plating in the case of bacteria and qPCR in the case of virus, respectively.

5.3 Results and Discussion

5.3.1 Evaluation of cell washing efficiency for plastic bead clearance

As a proof-of-concept experiment for adventitious agent clearance using spiral inertial microfluidic sorter, fluorescent polystyrene (PS) beads with 1- μm diameter were spiked into a 5-mL CHO cell culture sample with $\sim 2.07 \times 10^6$ cells/mL, and cell washing was performed until a fresh medium of 10 times initial sample volume (50 mL) was added to the initial sample (Fig. 16a). The concentration of PS beads in the sample was reduced from $\sim 4.22 \times 10^7$ beads/mL (initial) to $\sim 1.00 \times 10^4$ beads/mL (after 50mL washing) (Fig. 16d), which demonstrated the clearance level of 3.62 LRV ($\sim 4,170$ -fold) while 54.6% CHO cells were retained in the sample (Fig. 16c). The viability of the CHO cell was maintained throughout the washing operation (Fig. 16b).

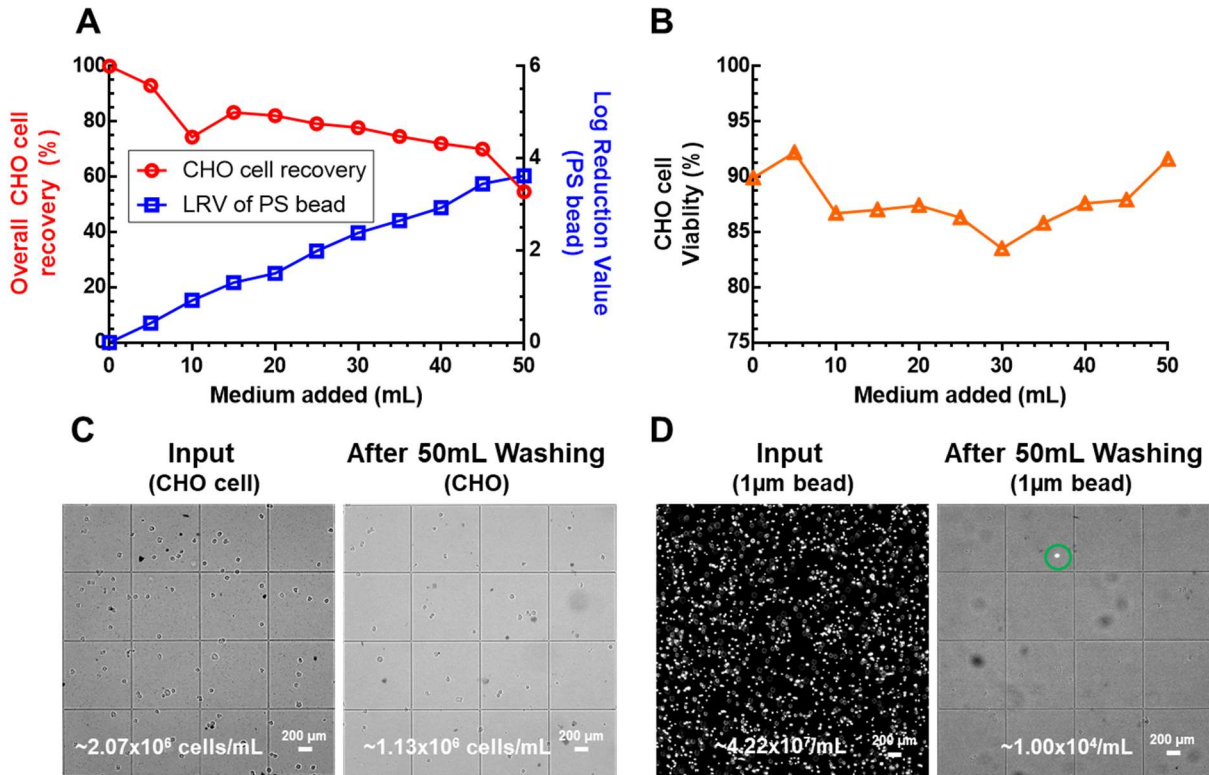


Figure 34 (A) CHO cell recovery (left y-axis, red symbol) and log reduction value (LRV) of 1 μm polystyrene beads (right y-axis, blue symbol) vs. medium volume added during spiral microfluidic sorter operation with constant medium addition scheme (B) CHO cell viability during spiral microfluidics cell washing operation (C) Bright-field microscopic images of the initial input and the final sample (washed

with 50 mL of medium) for comparison of CHO cell concentration (D) Fluorescence microscopic image of the initial input and the final sample for comparison of 1 μ m beads concentration.

5.3.2 Evaluation of cell washing efficiency for bacterial clearance

To demonstrate bacterial adventitious agent clearance, we spiked bacteria (GFP *E.coli*) with a concentration of $\sim 2.81 \times 10^8$ CFU/mL into a CHO cell sample of 10 mL with a total cell concentration of $\sim 1.26 \times 10^6$ cells/mL and processed the mixed sample with our spiral microfluidics with constant medium addition. As shown in Fig. 17a, CHO cell recovery of ~ 72.1 % (final $\sim 9.05 \times 10^5$ cells/mL) was achieved after 150 mL washing with a sterile medium compared with the initial input, while the concentration of *E. coli* was reduced by 4.32 LRV ($\sim 20,900$ -fold). It was confirmed that viability was not affected by spiral washing operation (Fig. 17b&c). There were $\sim 1.36 \times 10^4$ CFU/mL *E.coli* left in the final sample, confirmed by fluorescence microscopy and CFU plating on Luria-Bertani (LB) agar plate (Fig. 17d). The LRV of *E.coli* started to become saturated around ~ 4 LRV and increased slowly after 100 mL washing medium addition. This was because some portion of *E.coli* adhered to the CHO cells, and they were retained along with CHO cells in the spiral feedback loop.

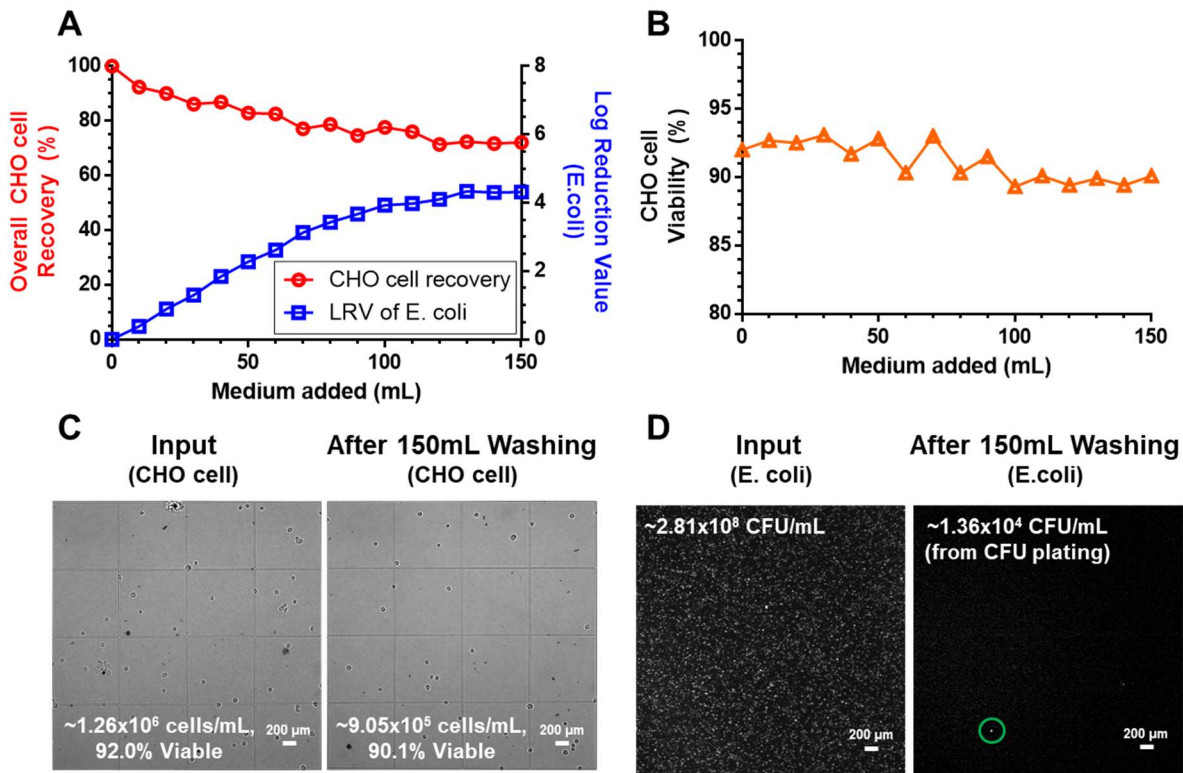


Figure 35 (A) CHO cell recovery (left y-axis, red symbol) and log reduction value (LRV) of *E. coli* (right y-axis, blue symbol) vs. medium volume added during spiral microfluidic sorter operation with constant medium addition scheme (B) CHO cell viability during spiral microfluidics cell washing operation for bacterial clearance (C) Bright-field microscopic images of the initial input and the final sample (washed with 150 mL of medium) for comparison of CHO cell concentration (D) Fluorescence microscopic image of the initial input and the final sample for comparison of *E. coli* concentration.

5.3.3 Evaluation of cell washing efficiency for viral clearance

For the virus clearance experiment, three 10-mL CHO cell culture samples with a cell concentration range of ~ 2.19 - 3.84×10^6 cells/mL were prepared and spiked with MVM at a multiplicity of infection (MOI) of ~ 1 - 10 (CHO cell:MVM=1: ~ 1 - 10) so that there is enough number of viruses to infect cells and to be detected by qPCR as well. Since adherence of MVM to CHO cell was observed in our preliminary experiments (data not shown) and resulted in inefficient washing efficiency, neuraminidase treatment was adopted as a method to minimize viral adherence by removing sialic acids on the cell membrane, which functions as the viral receptor. As shown in Fig. 18a, the overall

recovery of CHO cells was higher than 60% for all samples, including control and neuraminidase-treated samples. However, regarding the viral clearance performance, neuraminidase-treated samples (incubated with 20 mU/mL and 100 mU/mL neuraminidase) displayed approximately one order higher viral clearance compared to the control (non-treated) sample after the samples were continuously washed with 100 mL of medium (Fig. 18b). The neuraminidase-treated samples resulted in LRV of 2.03 and 1.92 after 100 mL cell washing for 20 mU/mL and 100 mU/mL neuraminidase treatments, respectively, while the control only had LRV of 0.98. The viability of CHO cells in all three samples was maintained almost constant (less than 6% variation) (Fig. 18c). This implies that neuraminidase treatment effectively reduced the number of viral receptors (sialic acids, supposedly) by one order of magnitude and enhanced the viral clearance performance significantly. However, the efficacy of spiral cell washing for viral adventitious agent clearance was less effective (about 2 LRV less) compared with other adventitious agent clearance experiments such as plastic beads and bacteria at the same level of washing (10 times the volume of washing medium with respect to the initial sample). Based on the fact that one neuraminidase treatment may not be able to remove all sialic acids and other potential viral receptors on the cell membrane, it is understood that the reduced efficacy of spiral cell washing for viral clearance results from viral adherence to receptors that still exist after neuraminidase treatment.

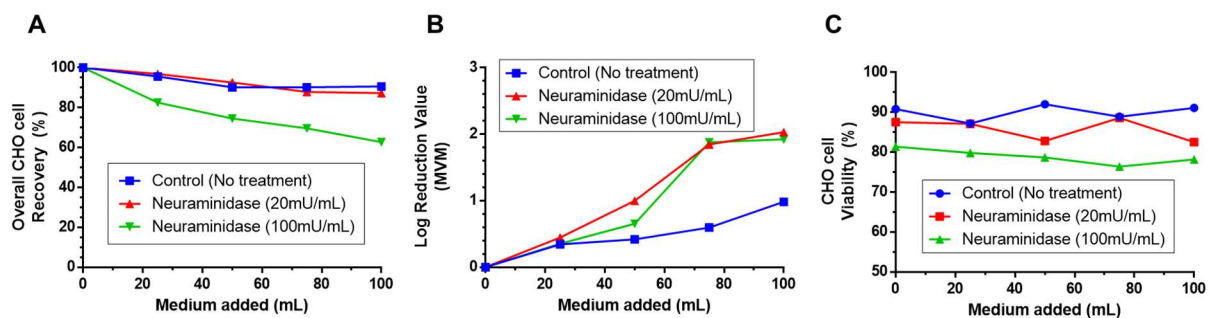


Figure 36 (A) CHO cell recovery vs. added washing medium volume graph for three samples with different treatment conditions during spiral microfluidics cell washing (B) Log reduction value (LRV) of MVM vs. added washing medium volume graph for three samples with different treatment conditions (C) CHO cell viability of three samples with different treatment conditions during spiral microfluidics cell washing operation for viral clearance.

5.3.4 Area of Application for Spiral-based Cell Washing Technology

Spiral microfluidic cell sorter can be readily applied as a cell washing method to wash mammalian cells for biologics production (*e.g.*, CHO cells) before cell culture as it can exchange the buffer to a fresh medium, removing residual metabolites or contaminants in the cell bank by orders of magnitudes without affecting cell viability. Operation of the spiral-based cell washing can be accomplished in a fully closed and automated manner, thus does not require any centrifugation and decanting step that might be prone to human error or lead to exposure of the sample to the external environment. Although it is unlikely that the cell bank had been contaminated before expansion, it would be better to have another layer of clearance at upstream bioprocessing.

Spiral-based cell washing can also be applied as a downstream adventitious agent clearance method for cell therapy products by separating larger cells from smaller adventitious agents such as bacteria and viruses. For example, CAR T-cells (approximate cell diameter of 5-7 μm ¹³²) differ in size from most common adventitious agents such as mycoplasma (diameter of 0.2-0.3 μm ¹³³) or replication-competent retrovirus (RCR) (diameter of 100 nm¹³⁴), thus can be hydrodynamically focused at one side of the spiral microchannel while adventitious agents are washed away and discarded at the other side, the waste outlet of the spiral microfluidic sorter. Cell washing can be continued repeatedly as long as the fresh medium is replenished until desired safety level of clearance (log reduction) is achieved.

Another potential area of application for spiral-based cell washing technology is viral vector production. Our group already demonstrated our spiral microfluidic cell sorter could be used as a cell retention device for perfusion mammalian cell culture for continuous monoclonal antibody production.^{49,129} We have also shown that our spiral device can separate viruses from a blood sample with high recovery (>95%) in another paper.³ Combining these two concepts, we can devise a viral vector production system where viral vectors are produced by transfected/transduced cells while they are grown within a bioreactor connected with a spiral sorter as a cell retention device.

5.3.5 Comparison with Currently Available Technology

Alternating tangential flow filtration (ATF) and tangential flow filtration (TFF) are deemed efficient and effective cell retention technology and are being adopted as a way to retain either mammalian cells¹¹⁶ or separate expanded mesenchymal stem cells (MSCs) out from microcarriers that are used to culture them.¹³⁵ However, membrane filtration technology suffers from its inevitable problem of membrane fouling and clogging, which degrades its efficiency over time, thus necessitates replacement. Moreover, the size of the mesh is fixed so that it is either too small for some adventitious agents to exit from the culture or too large for selective separation of cell and adventitious agents to occur. Spiral-based cell washing is the only technology that enables the clearance of bacteria as well as viruses at the same time in a single platform.

Another technology called acoustic wave separation can clarify harvested cell culture fluid continuously¹³⁶ or wash and concentrate cellular products in cell therapy manufacturing.¹⁰⁰ However, this technology is limited in the way that it induces aggregation of cells during the process, and the cells need to be dispersed later, which might cause undesirable additional shear stress on cells. Although much improvement is being made regarding how to induce cell aggregation more efficiently without affecting cell viability and functionality, it is pointed out that this technology normally requires high-density cell samples ($> 2 \times 10^7$ cells/mL), which is higher than typical mammalian cell culture as an input.^{100,137} Spiral-based cell washing is an aggregation-free cell washing technology without any restriction on the cell density of the input sample.

Centrifugation or counterflow centrifugation technology is also considered as another candidate for cell washing and concentration. Although being developed with meticulous engineering on fluidic control and chamber design, it is thought that its scalability is somewhat limited by the volume of the chamber as process scale would be mainly determined by the chamber size where maximum packed volume can reside. On the contrary, the spiral device can be fabricated with multiple vertical stacks for easy scale-up using the same footprint.^{22,51}

5.4 Chapter Conclusion

A spiral microfluidic sorter-based membrane-less, continuous, automated cell washing system was developed for adventitious agent clearance in cellular samples and products in biomanufacturing. Adventitious agents such as bacteria and viruses were efficiently removed by adding a fresh medium continuously to an adventitious agents-containing sample while the cells of interest were retained in the feedback loop of the spiral microfluidic sorter. Since the sorting mechanism of this system is purely based on the balance of hydrodynamic forces in the spiral microchannel, this system does not necessitate the use of a membrane, which might lead to fouling and clogging of the membrane, thus complete shutdown of the operation in the long run. Moreover, this cell washing method is beneficial for overall cell health because it does not induce any aggregation like other cell washing methods such as centrifugation and acoustic wave separation by its nature. In addition, it can also significantly reduce the chance of adventitious agent contamination incurring from human error by its automated operation. Also, the scalability of this system will enable versatile applications of this system from small-scale cell therapy products to large-volume bio-products. To our best knowledge, there is no such device or method that can be used to separate more than one kind of adventitious agent continuously with a single platform without inducing a change of cell morphology except for our spiral microfluidic sorter. We deem our spiral sorter-based cell washing/concentration not only promising for both upstream and downstream bioprocessing but also unique in that it makes what was thought to be impossible possible.

Chapter 6

Conclusion and Outlook

We have shown how a spiral microfluidic cell sorting device was used to prepare viral blood samples to isolate virus particles from host blood cells in whole blood or plasma samples and enhanced the metagenomic sequencing data by reducing the number of background (human) reads (Chapter 2). Not only was our spiral cell sorter able to improve viral genome coverage depth for the processed samples at the same level of sequencing depth compared to the unprocessed ones, but it was also shown that this improvement was more distinctive in lower tittered viral samples, which suggests that our technology would be more effectively used for enhancing the sensitivity of sequencing-based viral detection where viral titers are expected to be very low. Some blood lysis techniques were introduced and compared for their efficacy in recovering bacteria from clinical bacteremic blood samples without affecting much of their viability (Chapter 3). Although these blood lysis techniques have not been directly adopted for any downstream assays yet, we find them readily applicable to clinical blood sample preparation for diagnostic purposes, possibly in conjunction with spiral microfluidic cell sorter processing. We have also demonstrated low abundance bacteria detection from spiked blood samples down to ~1-5 CFU/mL level without any amplification method applied (*e.g.*, PCR or blood culture) by using a spiral microfluidic cell sorter as a sample preparation device that isolates bacteria from blood cells and an electrokinetic concentrator as a detection device where rRNA-probe conjugate is concentrated and detected with fluorescence microscopy. (Chapter 4) Since the process does not require any lengthy procedures such as culture or PCR, we were able to shorten the entire process from sample preparation to detection within an hour. We anticipate this process could be

further expedited if integrated with an automated cell concentration device and enable faster diagnosis of BSI without requiring a complicated, high-profile analyzer at the downstream side. As this process is free from usual sample preparation procedures that might cause false positives or amplification bias, it would also enable detection of polymicrobial bacteremia with the help of multiplexed probe set. Lastly, we have applied our spiral cell sorting technology as a continuous cell washing method for adventitious agent clearance in mammalian cell culture samples in biomanufacturing (Chapter 5). We were able to demonstrate reduction of adventitious agents such as bacteria and virus from spiked samples by 2-4 logs without affecting cell viability and inducing morphological change, thus guaranteeing overall cell health and quality. This cell washing technique can be readily applied to the upstream biomanufacturing process where cell banks are washed before cell culture to exchange the buffer to a fresh medium and remove residual metabolites and potential adventitious agents in them. Also, it can be used as a downstream clearance method for cell therapy products such as CAR T cells as these cells are usually larger than most common adventitious agents and can be easily separated using spiral cell sorting. Overall, there have been numerous biological applications developed for various types of biological samples, including the examples presented in my thesis, and yet there remain many other potential areas where they can benefit from the ability of spiral cell sorting technology to enhance sample purity. We envision that our spiral cell sorting technology would be applied as a versatile tool that can provide a way to better prepare biological samples for faster and more sensitive diagnosis as well as a more efficient production method for biomanufacturing products with better quality.

Bibliography

- (1) Kim, J.; Johnson, M.; Hill, P.; Gale, B. K. Microfluidic Sample Preparation: Cell Lysis and Nucleic Acid Purification. *Integr. Biol.* **2009**, *1* (10), 574–586.
<https://doi.org/10.1039/b905844c>.
- (2) Cui, F.; Rhee, M.; Singh, A.; Tripathi, A. Microfluidic Sample Preparation for Medical Diagnostics. *Annu. Rev. Biomed. Eng.* **2015**, *17* (1), 267–286.
<https://doi.org/10.1146/annurev-bioeng-071114-040538>.
- (3) Choi, K.; Ryu, H.; Siddle, K. J.; Piantadosi, A.; Freimark, L.; Park, D. J.; Sabeti, P.; Han, J. Negative Selection by Spiral Inertial Microfluidics Improves Viral Recovery and Sequencing from Blood. *Anal. Chem.* **2018**, *90* (7), 4657–4662.
<https://doi.org/10.1021/acs.analchem.7b05200>.
- (4) Ryu, H.; Choi, K.; Qu, Y.; Kwon, T.; Lee, J. S.; Han, J. Patient-Derived Airway Secretion Dissociation Technique To Isolate and Concentrate Immune Cells Using Closed-Loop Inertial Microfluidics. *Anal. Chem.* **2017**, *89* (10), 5549–5556.
<https://doi.org/10.1021/acs.analchem.7b00610>.
- (5) Chakraborty, S. P.; Karmahapatra, S. Isolation and Identification of Vancomycin Resistant Staphylococcus Aureus from Post Operative Pus Sample. *Aus Natl. Libr. Med. enllisted J.* **2011**, *4* (2), 152–168.
- (6) Koh, C. Y.; Schaff, U. Y.; Piccini, M. E.; Stanker, L. H.; Cheng, L. W.; Ravichandran, E.; Singh, B. R.; Sommer, G. J.; Singh, A. K. Centrifugal Microfluidic Platform for Ultrasensitive Detection of Botulinum Toxin. *Anal. Chem.* **2015**, *87* (2), 922–928.
<https://doi.org/10.1021/ac504054u>.
- (7) Schaff, U. Y.; Sommer, G. J. Whole Blood Immunoassay Based on Centrifugal Bead Sedimentation. *Clin. Chem.* **2011**, *57* (5), 753–761.
<https://doi.org/10.1373/clinchem.2011.162206>.
- (8) Cho, Y. K.; Lee, J. G.; Park, J. M.; Lee, B. S.; Lee, Y.; Ko, C. One-Step Pathogen Specific DNA Extraction from Whole Blood on a Centrifugal Microfluidic Device. *Lab Chip* **2007**, *7* (5), 565–573. <https://doi.org/10.1039/b616115d>.
- (9) Park, J.; Sunkara, V.; Kim, T. H.; Hwang, H.; Cho, Y. K. Lab-on-a-Disc for Fully

- Integrated Multiplex Immunoassays. *Anal. Chem.* **2012**, *84* (5), 2133–2140.
<https://doi.org/10.1021/ac203163u>.
- (10) Srinivasan, V.; Pamula, V. K.; Fair, R. B. An Integrated Digital Microfluidic Lab-on-a-Chip for Clinical Diagnostics on Human Physiological Fluids. *Lab Chip* **2004**, *4* (4), 310–315. <https://doi.org/10.1039/b403341h>.
- (11) Wheeler, A. R.; Moon, H.; Kim, C. J.; Loo, J. A.; Garrell, R. L. Electrowetting-Based Microfluidics for Analysis of Peptides and Proteins by Matrix-Assisted Laser Desorption/Ionization Mass Spectrometry. *Anal. Chem.* **2004**, *76* (16), 4833–4838.
<https://doi.org/10.1021/ac0498112>.
- (12) Chang, Y. H.; Lee, G. Bin; Huang, F. C.; Chen, Y. Y.; Lin, J. L. Integrated Polymerase Chain Reaction Chips Utilizing Digital Microfluidics. *Biomed. Microdevices* **2006**, *8* (3), 215–225. <https://doi.org/10.1007/s10544-006-8171-y>.
- (13) Mousa, N. A.; Jebrail, M. J.; Yang, H.; Abdelgawad, M.; Metalnikov, P.; Chen, J.; Wheeler, A. R.; Casper, R. F. Droplet-Scale Estrogen Assays in Breast Tissue, Blood, and Serum. *Sci. Transl. Med.* **2009**, *1* (1), 1ra2-1ra2.
<https://doi.org/10.1126/scitranslmed.3000105>.
- (14) Dimov, I. K.; Basabe-Desmots, L.; Garcia-Cordero, J. L.; Ross, B. M.; Ricco, A. J.; Lee, L. P.; Kwong, G. A.; Liu, C.-C.; Gould, J.; Hood, L.; et al. Stand-Alone Self-Powered Integrated Microfluidic Blood Analysis System (SIMBAS). *Lab Chip* **2011**, *11* (5), 845–850. <https://doi.org/10.1039/C0LC00403K>.
- (15) Zhang, X.-B.; Wu, Z.-Q.; Wang, K.; Zhu, J.; Xu, J.-J.; Xia, X.-H.; Chen, H.-Y. Gravitational Sedimentation Induced Blood Delamination for Continuous Plasma Separation on a Microfluidics Chip. *Anal. Chem.* **2012**, *84* (8), 3780–3786.
<https://doi.org/10.1021/ac3003616>.
- (16) Pamme, N.; Manz, A. On-Chip Free-Flow Magnetophoresis: Continuous Flow Separation of Magnetic Particles and Agglomerates. *Anal. Chem.* **2004**, *76* (24), 7250–7256.
<https://doi.org/10.1021/ac049183o>.
- (17) Pamme, N.; Wilhelm, C. Continuous Sorting of Magnetic Cells via On-Chip Free-Flow Magnetophoresis. *Lab Chip* **2006**, *6* (8), 974–980. <https://doi.org/10.1039/b604542a>.
- (18) Hale, C.; Darabi, J. Magnetophoretic-Based Microfluidic Device for DNA Isolation.

- Biomicrofluidics* **2014**, *8* (4), 044118. <https://doi.org/10.1063/1.4893772>.
- (19) Karle, M.; Miwa, J.; Czilwik, G.; Auwärter, V.; Roth, G.; Zengerle, R.; Von Stetten, F. Continuous Microfluidic DNA Extraction Using Phase-Transfer Magnetophoresis. *Lab Chip* **2010**, *10* (23), 3284–3290. <https://doi.org/10.1039/c0lc00129e>.
- (20) Kuntaegowdanahalli, S. S.; Bhagat, A. A. S.; Kumar, G.; Papautsky, I.; Quake, S. R.; Scrivens, W. A.; Kim, K. S. Inertial Microfluidics for Continuous Particle Separation in Spiral Microchannels. *Lab Chip* **2009**, *9* (20), 2973. <https://doi.org/10.1039/b908271a>.
- (21) Wu, L.; Guan, G.; Hou, H. W.; Bhagat, A. A. S.; Han, J. Separation of Leukocytes from Blood Using Spiral Channel with Trapezoid Cross-Section. *Anal. Chem.* **2012**, *84* (21), 9324–9331. <https://doi.org/10.1021/ac302085y>.
- (22) Warkiani, M. E.; Khoo, B. L.; Wu, L.; Tay, A. K. P.; Bhagat, A. A. S.; Han, J.; Lim, C. T. Ultra-Fast, Label-Free Isolation of Circulating Tumor Cells from Blood Using Spiral Microfluidics. *Nat. Protoc.* **2015**, *11* (1), 134–148. <https://doi.org/10.1038/nprot.2016.003>.
- (23) Hou, H. W.; Bhattacharyya, R. P.; Hung, D. T.; Han, J. Direct Detection and Drug-Resistance Profiling of Bacteremias Using Inertial Microfluidics. *Lab Chip* **2015**, *15* (10), 2297–2307. <https://doi.org/10.1039/c5lc00311c>.
- (24) Son, J.; Samuel, R.; Gale, B. K.; Carrell, D. T.; Hotaling, J. M. Separation of Sperm Cells from Samples Containing High Concentrations of White Blood Cells Using a Spiral Channel. *Biomicrofluidics* **2017**, *11* (5), 054106. <https://doi.org/10.1063/1.4994548>.
- (25) Liu, C.; Mauk, M.; Gross, R.; Bushman, F. D.; Edelstein, P. H.; Collman, R. G.; Bau, H. H. Membrane-Based, Sedimentation-Assisted Plasma Separator for Point-of-Care Applications. *Anal. Chem.* **2013**, *85* (21), 10463–10470. <https://doi.org/10.1021/ac402459h>.
- (26) Wang, S. Q.; Sarenac, D.; Chen, M. H.; Huang, S. H.; Giguel, F. F.; Kuritzkes, D. R.; Demirci, U. Simple Filter Microchip for Rapid Separation of Plasma and Viruses from Whole Blood. *Int. J. Nanomedicine* **2012**, *7*, 5019–5028. <https://doi.org/10.2147/IJN.S32579>.
- (27) Haeberle, S.; Brenner, T.; Zengerle, R.; Ducrée, J. Centrifugal Extraction of Plasma from Whole Blood on a Rotating Disk. *Lab Chip* **2006**, *6* (6), 776–781. <https://doi.org/10.1039/B604145K>.

- (28) Gorkin, R.; Park, J.; Siegrist, J.; Amasia, M.; Lee, B. S.; Park, J.-M.; Kim, J.; Kim, H.; Madou, M.; Cho, Y.-K.; et al. Centrifugal Microfluidics for Biomedical Applications. *Lab Chip* **2010**, *10* (14), 1758. <https://doi.org/10.1039/b924109d>.
- (29) CHEN, X.; CUI, D.; LIU, C.; LI, H. Microfluidic Chip for Blood Cell Separation and Collection Based on Crossflow Filtration. *Sensors Actuators B Chem.* **2008**, *130* (1), 216–221. <https://doi.org/10.1016/j.snb.2007.07.126>.
- (30) Vandelinder, V.; Groisman, A. Separation of Plasma from Whole Human Blood in a Continuous Cross-Flow in a Molded Microfluidic Device. *Anal. Chem.* **2006**, *78*, 3765–3771. <https://doi.org/10.1021/ac060042r>.
- (31) Tachi, T.; Kaji, N.; Tokeshi, M.; Baba, Y. Simultaneous Separation, Metering, and Dilution of Plasma from Human Whole Blood in a Microfluidic System. *Anal. Chem.* **2009**, *81* (8), 3194–3198. <https://doi.org/10.1021/ac802434z>.
- (32) Ngoi, C. N.; Siqueira, J.; Li, L.; Deng, X.; Mugo, P.; Graham, S. M.; Price, M. A.; Sanders, E. J.; Delwart, E. The Plasma Virome of Febrile Adult Kenyans Shows Frequent Parvovirus B19 Infections and a Novel Arbovirus (Kadipiro Virus). *J. Gen. Virol.* **2016**, *97* (12), 3359–3367. <https://doi.org/10.1099/jgv.0.000644>.
- (33) Wilson, M. R.; Zimmermann, L. L.; Crawford, E. D.; Sample, H. A.; Soni, P. R.; Baker, A. N.; Khan, L. M.; DeRisi, J. L. Acute West Nile Virus Meningoencephalitis Diagnosed Via Metagenomic Deep Sequencing of Cerebrospinal Fluid in a Renal Transplant Patient. *Am. J. Transplant.* **2017**, *17* (3), 803–808. <https://doi.org/10.1111/ajt.14058>.
- (34) Grard, G.; Fair, J. N.; Lee, D.; Slikas, E.; Steffen, I.; Muyembe, J.-J.; Sittler, T.; Veeraraghavan, N.; Ruby, J. G.; Wang, C.; et al. A Novel Rhabdovirus Associated with Acute Hemorrhagic Fever in Central Africa. *PLoS Pathog.* **2012**, *8* (9), e1002924. <https://doi.org/10.1371/journal.ppat.1002924>.
- (35) McMullan, L. K.; Folk, S. M.; Kelly, A. J.; MacNeil, A.; Goldsmith, C. S.; Metcalfe, M. G.; Batten, B. C.; Albariño, C. G.; Zaki, S. R.; Rollin, P. E.; et al. A New Phlebovirus Associated with Severe Febrile Illness in Missouri. *N. Engl. J. Med.* **2012**, *367* (9), 834–841. <https://doi.org/10.1056/NEJMoa1203378>.
- (36) Kosoy, O. I.; Lambert, A. J.; Hawkinson, D. J.; Pastula, D. M.; Goldsmith, C. S.; Hunt, D. C.; Staples, J. E. Novel Thogotovirus Associated with Febrile Illness and Death, United

- States, 2014. *Emerg. Infect. Dis.* **2015**, *21* (5), 760–764.
<https://doi.org/10.3201/eid2105.150150>.
- (37) Stremlau, M. H.; Andersen, K. G.; Folarin, O. A.; Grove, J. N.; Odia, I.; Ehiane, P. E.; Omoniwa, O.; Omoregie, O.; Jiang, P.-P.; Yozwiak, N. L.; et al. Discovery of Novel Rhabdoviruses in the Blood of Healthy Individuals from West Africa. *PLoS Negl. Trop. Dis.* **2015**, *9* (3), e0003631. <https://doi.org/10.1371/journal.pntd.0003631>.
- (38) Gire, S. K.; Goba, A.; Andersen, K. G.; Sealfon, R. S. G.; Park, D. J.; Kanneh, L.; Jalloh, S.; Momoh, M.; Fullah, M.; Dudas, G.; et al. Genomic Surveillance Elucidates Ebola Virus Origin and Transmission during the 2014 Outbreak. *Science* **2014**, *345* (6202), 1369–1372. <https://doi.org/10.1126/science.1259657>.
- (39) Park, D. J.; Dudas, G.; Wohl, S.; Goba, A.; Whitmer, S. L. M.; Andersen, K. G.; Sealfon, R. S.; Ladner, J. T.; Kugelman, J. R.; Matranga, C. B.; et al. Ebola Virus Epidemiology, Transmission, and Evolution during Seven Months in Sierra Leone. *Cell* **2015**, *161* (7), 1516–1526. <https://doi.org/10.1016/j.cell.2015.06.007>.
- (40) Matranga, C. B.; Andersen, K. G.; Winnicki, S.; Busby, M.; Gladden, A. D.; Tewhey, R.; Stremlau, M.; Berlin, A.; Gire, S. K.; England, E.; et al. Enhanced Methods for Unbiased Deep Sequencing of Lassa and Ebola RNA Viruses from Clinical and Biological Samples. *Genome Biol.* **2014**, *15* (11), 519. <https://doi.org/10.1186/PREACCEPT-1698056557139770>.
- (41) Gu, W.; Crawford, E. D.; O'Donovan, B. D.; Wilson, M. R.; Chow, E. D.; Retallack, H.; DeRisi, J. L. Depletion of Abundant Sequences by Hybridization (DASH): Using Cas9 to Remove Unwanted High-Abundance Species in Sequencing Libraries and Molecular Counting Applications. *Genome Biol.* **2016**, *17* (1), 41. <https://doi.org/10.1186/s13059-016-0904-5>.
- (42) Rios, M.; Daniel, S.; Chancey, C.; Hewlett, I. K.; Stramer, S. L. West Nile Virus Adheres to Human Red Blood Cells in Whole Blood. *Clin. Infect. Dis.* **2007**, *45* (2), 181–186. <https://doi.org/10.1086/518850>.
- (43) Lustig, Y.; Mannasse, B.; Koren, R.; Katz-Likvornik, S.; Hindiyeh, M.; Mandelboim, M.; Dovrat, S.; Sofer, D.; Mendelson, E. Superiority of West Nile Virus RNA Detection in Whole Blood for Diagnosis of Acute Infection. *J. Clin. Microbiol.* **2016**, *54* (9), 2294–

2297. <https://doi.org/10.1128/JCM.01283-16>.
- (44) Shim, J. S.; Ahn, C. H.; Beaucage, G.; Nevin, J. H.; Lee, J.-B.; Puntambekar, A.; Lee, J. Y.; Liu, C.; Gould, J.; Hood, L.; et al. An On-Chip Whole Blood/Plasma Separator Using Hetero-Packed Beads at the Inlet of a Microchannel. *Lab Chip* **2012**, *12* (5), 863. <https://doi.org/10.1039/c2lc21009f>.
- (45) Lee, K. K.; Ahn, C. H.; Schmitt, J.; Nevin, J. H.; Lee, J.-B.; Puntambekar, A.; Lee, J. Y.; Lilja, H.; Laurell, T.; Hood, L.; et al. A New On-Chip Whole Blood/Plasma Separator Driven by Asymmetric Capillary Forces. *Lab Chip* **2013**, *13* (16), 3261. <https://doi.org/10.1039/c3lc50370d>.
- (46) Di Carlo, D.; Irimia, D.; Tompkins, R. G.; Toner, M. Continuous Inertial Focusing, Ordering, and Separation of Particles in Microchannels. *Proc. Natl. Acad. Sci. U. S. A.* **2007**, *104* (48), 18892–18897. <https://doi.org/10.1073/pnas.0704958104>.
- (47) Bhagat, A. A. S.; Kuntaegowdanahalli, S. S.; Papautsky, I. Inertial Microfluidics for Continuous Particle Filtration and Extraction. *Microfluid. Nanofluidics* **2009**, *7* (2), 217–226. <https://doi.org/10.1007/s10404-008-0377-2>.
- (48) Di Carlo, D. Inertial Microfluidics. *Lab Chip* **2009**, *9* (21), 3038–3046. <https://doi.org/10.1039/b912547g>.
- (49) Warkiani, M. E.; Tay, A. K. P.; Guan, G.; Han, J. Membrane-Less Microfiltration Using Inertial Microfluidics. *Sci. Rep.* **2015**, *5*, 11018.
- (50) Warkiani, M. E.; Wu, L.; Tay, A. K. P.; Han, J. Large-Volume Microfluidic Cell Sorting for Biomedical Applications. *Annu. Rev. Biomed. Eng.* **2015**, *17* (1), 1–34. <https://doi.org/10.1146/annurev-bioeng-071114-040818>.
- (51) Rafeie, M.; Zhang, J.; Asadnia, M.; Li, W.; Warkiani, M. E.; Ni, Z.; Ni, Z.; Han, J.; Han, J.; Lim, C. T. Multiplexing Slanted Spiral Microchannels for Ultra-Fast Blood Plasma Separation. *Lab Chip* **2016**, *16* (15), 2791–2802. <https://doi.org/10.1039/C6LC00713A>.
- (52) Salafi, T.; Zeming, K. K.; Zhang, Y. Advancements in Microfluidics for Nanoparticle Separation. *Lab Chip* **2017**, *17* (1), 11–33. <https://doi.org/10.1039/C6LC01045H>.
- (53) Peres, R. M. B.; Costa, C. R. C.; Andrade, P. D.; Bonon, S. H. A.; Albuquerque, D. M.; de Oliveira, C.; Vigorito, A. C.; Aranha, F. J. P.; de Souza, C. A.; Costa, S. C. B. Surveillance of Active Human Cytomegalovirus Infection in Hematopoietic Stem Cell

- Transplantation (HLA Sibling Identical Donor): Search for Optimal Cutoff Value by Real-Time PCR. *BMC Infect. Dis.* **2010**, *10*, 147. <https://doi.org/10.1186/1471-2334-10-147>.
- (54) Wood, D. E.; Salzberg, S. L. Kraken: Ultrafast Metagenomic Sequence Classification Using Exact Alignments. *Genome Biol.* **2014**, *15* (3), R46. <https://doi.org/10.1186/gb-2014-15-3-r46>.
- (55) Metsky, H. C.; Matranga, C. B.; Wohl, S.; Schaffner, S. F.; Freije, C. A.; Winnicki, S. M.; West, K.; Qu, J.; Baniecki, M. L.; Gladden-Young, A.; et al. Zika Virus Evolution and Spread in the Americas. *Nature* **2017**, *546* (7658), 411–415. <https://doi.org/10.1038/nature22402>.
- (56) Svanes, K.; Zweifach, B. W. Variations in Small Blood Vessel Hematocrits Produced in Hypothermic Rats by Micro-Occlusion. *Microvasc. Res.* **1968**, *1* (2), 210–220. [https://doi.org/10.1016/0026-2862\(68\)90019-8](https://doi.org/10.1016/0026-2862(68)90019-8).
- (57) Fung, Y.-C. Stochastic Flow in Capillary Blood Vessels. *Microvasc. Res.* **1973**, *5* (1), 34–48. [https://doi.org/10.1016/S0026-2862\(73\)80005-6](https://doi.org/10.1016/S0026-2862(73)80005-6).
- (58) Henry, N. K.; McLimans, C. A.; Wright, A. J.; Thompson, R. L.; Wilson, W. R.; Washington, J. A. Microbiological and Clinical Evaluation of the Isolator Lysis-Centrifugation Blood Culture Tube. *J. Clin. Microbiol.* **1983**, *17* (5), 864–869.
- (59) Kreger, B. E.; Craven, D. E.; Carling, P. C.; McCabe, W. R. Gram-Negative Bacteremia. III. Reassessment of Etiology, Epidemiology and Ecology in 612 Patients. *Am. J. Med.* **1980**, *68* (3), 332–343. [https://doi.org/10.1016/0002-9343\(80\)90101-1](https://doi.org/10.1016/0002-9343(80)90101-1).
- (60) Opota, O.; Croxatto, A.; Prod'hom, G.; Greub, G. Blood Culture-Based Diagnosis of Bacteraemia: State of the Art. *Clin. Microbiol. Infect.* **2015**, *21* (4), 313–322. <https://doi.org/10.1016/J.CMI.2015.01.003>.
- (61) Opota, O.; Jatou, K.; Greub, G. Microbial Diagnosis of Bloodstream Infection: Towards Molecular Diagnosis Directly from Blood. *Clin. Microbiol. Infect.* **2015**, *21* (4), 323–331. <https://doi.org/10.1016/J.CMI.2015.02.005>.
- (62) Leitner, E.; Kessler, H. H.; Spindelboeck, W.; Hoenigl, M.; Putz-Bankuti, C.; Stadlbauer-Köllner, V.; Krause, R.; Grisold, A. J.; Feierl, G.; Stauber, R. E. Comparison of Two Molecular Assays with Conventional Blood Culture for Diagnosis of Sepsis. *J. Microbiol. Methods* **2013**, *92* (3), 253–255. <https://doi.org/10.1016/j.mimet.2012.12.012>.

- (63) Wellinghausen, N.; Kochem, A.-J.; Disqué, C.; Mühl, H.; Gebert, S.; Winter, J.; Matten, J.; Sakka, S. G. Diagnosis of Bacteremia in Whole-Blood Samples by Use of a Commercial Universal 16S rRNA Gene-Based PCR and Sequence Analysis. *J. Clin. Microbiol.* **2009**, *47* (9), 2759–2765. <https://doi.org/10.1128/JCM.00567-09>.
- (64) Wallet, F.; Nseir, S.; Baumann, L.; Herwegh, S.; Sendid, B.; Boulo, M.; Roussel-Delvallez, M.; Durocher, A. V.; Courcol, R. J. Preliminary Clinical Study Using a Multiplex Real-Time PCR Test for the Detection of Bacterial and Fungal DNA Directly in Blood. *Clin. Microbiol. Infect.* **2010**, *16* (6), 774–779. <https://doi.org/10.1111/j.1469-0691.2009.02940.x>.
- (65) Dark, P.; Wilson, C.; Blackwood, B.; McAuley, D. F.; Perkins, G. D.; McMullan, R.; Gates, S.; Warhurst, G. Accuracy of LightCycler® SeptiFast for the Detection and Identification of Pathogens in the Blood of Patients with Suspected Sepsis: A Systematic Review Protocol. *BMJ Open*. British Medical Journal Publishing Group January 1, 2012, p e000392. <https://doi.org/10.1136/bmjopen-2011-000392>.
- (66) Carrara, L.; Navarro, F.; Turbau, M.; Seres, M.; Morán, I.; Quintana, I.; Martino, R.; González, Y.; Brell, A.; Cordon, O.; et al. Molecular Diagnosis of Bloodstream Infections with a New Dual-Priming Oligonucleotide-Based Multiplex PCR Assay. *J. Med. Microbiol.* **2013**, *62* (PART 11), 1673–1679. <https://doi.org/10.1099/jmm.0.064758-0>.
- (67) Schreiber, J.; Nierhaus, A.; Braune, S. A.; de Heer, G.; Kluge, S. Vergleich Dreier Unterschiedlicher PCR-Testverfahren Zum Erregernachweis Bei Kritisch Kranken Patienten Mit Sepsis. *Medizinische Klin. - Intensivmed. und Notfallmedizin* **2013**, *108* (4), 311–318. <https://doi.org/10.1007/s00063-013-0227-1>.
- (68) Bacconi, A.; Richmond, G. S.; Baroldi, M. A.; Laffler, T. G.; Blyn, L. B.; Carolan, H. E.; Frinder, M. R.; Toleno, D. M.; Metzgar, D.; Gutierrez, J. R.; et al. Improved Sensitivity for Molecular Detection of Bacterial and Candida Infections in Blood. *J. Clin. Microbiol.* **2014**, *52* (9), 3164–3174. <https://doi.org/10.1128/JCM.00801-14>.
- (69) Jeng, K.; Gaydos, C. A.; Blyn, L. B.; Yang, S.; Won, H.; Matthews, H.; Toleno, D.; Hsieh, Y. H.; Carroll, K. C.; Hardick, J.; et al. Comparative Analysis of Two Broad-Range PCR Assays for Pathogen Detection in Positive-Blood-Culture Bottles: PCR-High-Resolution Melting Analysis versus PCR-Mass Spectrometry. *J. Clin. Microbiol.* **2012**, *50*

- (10), 3287–3292. <https://doi.org/10.1128/JCM.00677-12>.
- (70) De Angelis, G.; Posteraro, B.; De Carolis, E.; Menchinelli, G.; Franceschi, F.; Tumbarello, M.; De Pascale, G.; Spanu, T.; Sanguinetti, M. T2Bacteria Magnetic Resonance Assay for the Rapid Detection of ESKAPEc Pathogens Directly in Whole Blood. *J. Antimicrob. Chemother.* **2018**, *73* (suppl_4), iv20–iv26. <https://doi.org/10.1093/jac/dky049>.
- (71) Hong Nguyen, M.; Clancy, C. J.; William Pasculle, A.; Pappas, P. G.; Alangaden, G.; Pankey, G. A.; Schmitt, B. H.; Rasool, A.; Weinstein, M. P.; Widen, R.; et al. Performance of the T2bacteria Panel for Diagnosing Bloodstream Infections. *Ann. Intern. Med.* **2019**, *170* (12), 845–852. <https://doi.org/10.7326/M18-2772>.
- (72) Bhattacharyya, R. P.; Walker, M.; Boykin, R.; Son, S. S.; Liu, J.; Hachey, A. C.; Ma, P.; Wu, L.; Choi, K.; Cummins, K. C.; et al. Rapid Identification and Phylogenetic Classification of Diverse Bacterial Pathogens in a Multiplexed Hybridization Assay Targeting Ribosomal RNA. *Sci. Rep.* **2019**, *9* (1). <https://doi.org/10.1038/s41598-019-40792-3>.
- (73) Minasyan, H.; Flachsbart, F. Blood Coagulation: A Powerful Bactericidal Mechanism of Human Innate Immunity. *Int. Rev. Immunol.* **2019**, *38* (1), 3–17. <https://doi.org/10.1080/08830185.2018.1533009>.
- (74) Loof, T. G.; Deicke, C.; Medina, E. The Role of Coagulation/Fibrinolysis during *Streptococcus Pyogenes* Infection. *Front. Cell. Infect. Microbiol.* **2014**, *4* (SEP), 128. <https://doi.org/10.3389/fcimb.2014.00128>.
- (75) Sun, H. The Interaction Between Pathogens and the Host Coagulation System. *Physiology* **2006**, *21* (4), 281–288. <https://doi.org/10.1152/physiol.00059.2005>.
- (76) Baumann, E.; Stoya, G.; Völkner, A.; Richter, W.; Lemke, C.; Linss, W. Hemolysis of Human Erythrocytes with Saponin Affects the Membrane Structure. *Acta Histochem.* **2000**, *102* (1), 21–35. <https://doi.org/10.1078/0065-1281-00534>.
- (77) Dorn, G. L. DETOXIFICATION OF SAPONINS. U.S. Pat. 3883425A, 1975.
- (78) Anson, L. W.; Chau, K.; Sanderson, N.; Hoosdally, S.; Bradley, P.; Iqbal, Z.; Phan, H.; Foster, D.; Oakley, S.; Morgan, M.; et al. DNA Extraction from Primary Liquid Blood Cultures for Bloodstream Infection Diagnosis Using Whole Genome Sequencing. *J. Med.*

- Microbiol.* **2018**, *67* (3), 347–357. <https://doi.org/10.1099/jmm.0.000664>.
- (79) Kang, D.-K.; Ali, M. M.; Zhang, K.; Huang, S. S.; Peterson, E.; Digman, M. A.; Gratton, E.; Zhao, W. Rapid Detection of Single Bacteria in Unprocessed Blood Using Integrated Comprehensive Droplet Digital Detection. *Nat. Commun.* **2014**, *5*, 5427. <https://doi.org/10.1038/ncomms6427>.
- (80) Wen, J.; Legendre, L. A.; Bienvenue, J. M.; Landers, J. P. Purification of Nucleic Acids in Microfluidic Devices. *Analytical Chemistry*. American Chemical Society September 1, 2008, pp 6472–6479. <https://doi.org/10.1021/ac8014998>.
- (81) Yin, J.; Suo, Y.; Zou, Z.; Sun, J.; Zhang, S.; Wang, B.; Xu, Y.; Darland, D.; Zhao, J. X.; Mu, Y. Integrated Microfluidic Systems with Sample Preparation and Nucleic Acid Amplification. *Lab on a Chip*. Royal Society of Chemistry August 20, 2019, pp 2769–2785. <https://doi.org/10.1039/c9lc00389d>.
- (82) Bruijns, B.; van Asten, A.; Tiggelaar, R.; Gardeniers, H. Microfluidic Devices for Forensic DNA Analysis: A Review. *Biosensors* **2016**, *6* (3), 41. <https://doi.org/10.3390/bios6030041>.
- (83) Price, C. W.; Leslie, D. C.; Landers, J. P. Nucleic Acid Extraction Techniques and Application to the Microchip. *Lab on a Chip*. Royal Society of Chemistry September 7, 2009, pp 2484–2494. <https://doi.org/10.1039/b907652m>.
- (84) Petralia, S.; Sciuto, E. L.; Conoci, S. A Novel Miniaturized Biofilter Based on Silicon Micropillars for Nucleic Acid Extraction. *Analyst* **2017**, *142* (1), 140–146. <https://doi.org/10.1039/c6an02049f>.
- (85) Reedy, C. R.; Price, C. W.; Sniegowski, J.; Ferrance, J. P.; Begley, M.; Landers, J. P. Solid Phase Extraction of DNA from Biological Samples in a Post-Based, High Surface Area Poly(Methyl Methacrylate) (PMMA) Microdevice. *Lab Chip* **2011**, *11* (9), 1603–1611. <https://doi.org/10.1039/c0lc00597e>.
- (86) Witek, M. A.; Llopis, S. D.; Wheatley, A.; McCarley, R. L.; Soper, S. A. Purification and Preconcentration of Genomic DNA from Whole Cell Lysates Using Photoactivated Polycarbonate (PPC) Microfluidic Chips. *Nucleic Acids Res.* **2006**, *34* (10), e74–e74. <https://doi.org/10.1093/nar/gkl146>.
- (87) Bienvenue, J. M.; Legendre, L. A.; Ferrance, J. P.; Landers, J. P. An Integrated

- Microfluidic Device for DNA Purification and PCR Amplification of STR Fragments. *Forensic Sci. Int. Genet.* **2010**, *4* (3), 178–186.
<https://doi.org/10.1016/j.fsigen.2009.02.010>.
- (88) Hong, J. W.; Studer, V.; Hang, G.; Anderson, W. F.; Quake, S. R. A Nanoliter-Scale Nucleic Acid Processor with Parallel Architecture. *Nat. Biotechnol.* **2004**, *22* (4), 435–439. <https://doi.org/10.1038/nbt951>.
- (89) Ouyang, W.; Li, Z.; Han, J. Pressure-Modulated Selective Electrokinetic Trapping for Direct Enrichment, Purification, and Detection of Nucleic Acids in Human Serum. *Anal. Chem.* **2018**, *90* (19), 11366–11375. <https://doi.org/10.1021/acs.analchem.8b02330>.
- (90) Cheow, L. F.; Han, J. Continuous Signal Enhancement for Sensitive Aptamer Affinity Probe Electrophoresis Assay Using Electrokinetic Concentration. *Anal. Chem.* **2011**, *83* (18), 7086–7093. <https://doi.org/10.1021/ac201307d>.
- (91) Kwak, R.; Kim, S. J.; Han, J. Continuous-Flow Biomolecule and Cell Concentrator by Ion Concentration Polarization. *Anal. Chem.* **2011**, *83* (19), 7348–7355.
<https://doi.org/10.1021/ac2012619>.
- (92) Wang, Y. C.; Stevens, A. L.; Han, J. Million-Fold Preconcentration of Proteins and Peptides by Nanofluidic Filter. *Anal. Chem.* **2005**, *77* (14), 4293–4299.
<https://doi.org/10.1021/ac050321z>.
- (93) Ouyang, W.; Ko, S. H.; Wu, D.; Wang, A. Y.; Barone, P. W.; Hancock, W. S.; Han, J. Microfluidic Platform for Assessment of Therapeutic Proteins Using Molecular Charge Modulation Enhanced Electrokinetic Concentration Assays. *Anal. Chem.* **2016**, *88* (19), 9669–9677. <https://doi.org/10.1021/acs.analchem.6b02517>.
- (94) Brandenberger, R.; Burger, S.; Campbell, A.; Fong, T.; Lapinskas, E.; Rowley, J. A. Cell Therapy Bioprocessing <https://bioprocessintl.com/manufacturing/cell-therapies/cell-therapy-bioprocessing-314870/>.
- (95) Powell, D. J.; Brennan, A. L.; Zheng, Z.; Huynh, H.; Cotte, J.; Levine, B. L. Efficient Clinical-Scale Enrichment of Lymphocytes for Use in Adoptive Immunotherapy Using a Modified Counterflow Centrifugal Elutriation Program. *Cytotherapy* **2009**, *11* (7), 923–935. <https://doi.org/10.3109/14653240903188921>.
- (96) Coulais, D.; Panterne, C.; Fonteneau, J.-F.; Grégoire, M. Purification of Circulating

- Plasmacytoid Dendritic Cells Using Counterflow Centrifugal Elutriation and Immunomagnetic Beads. *Cytotherapy* **2012**, *14* (7), 887–896.
<https://doi.org/10.3109/14653249.2012.689129>.
- (97) Majore, I.; Moretti, P.; Hass, R.; Kasper, C. Identification of Subpopulations in Mesenchymal Stem Cell-like Cultures from Human Umbilical Cord. *Cell Commun. Signal.* **2009**, *7*, 6. <https://doi.org/10.1186/1478-811X-7-6>.
- (98) Li, A.; Wilson, S.; Fitzpatrick, I.; Barabadi, M.; Chan, S. T.; Krause, M.; Kusuma, G. D.; James, D.; Lim, R. Automated Counterflow Centrifugal System for Small-Scale Cell Processing. *JoVE* **2019**, No. 154, e60423. <https://doi.org/doi:10.3791/60423>.
- (99) Wegener, C.; Heber, C.; Min, K. Novel Cell Washing Device Using Spinning Membrane Filtration. *Cytotherapy* **2013**, *15* (4), S27. <https://doi.org/10.1016/J.JCYT.2013.01.102>.
- (100) Li, A.; Kusuma, G. D.; Driscoll, D.; Smith, N.; Wall, D. M.; Levine, B. L.; James, D.; Lim, R. Advances in Automated Cell Washing and Concentration. *Cytotherapy* **2021**. <https://doi.org/10.1016/j.jcyt.2021.04.003>.
- (101) Mungikar, A.; Kamat, M. Use of in-line Raman spectroscopy as a non-destructive and rapid analytical technique to monitor aggregation of a therapeutic protein <https://www.americanpharmaceuticalreview.com/Featured-Articles/37071-Use-of-In-line-Raman-Spectroscopy-as-a-Non-destructive-and-Rapid-Analytical-Technique-to-Monitor-Aggregation-of-a-Therapeutic-Protein/> (accessed Jun 4, 2021).
- (102) Ansorge, S.; Esteban, G.; Schmid, G. On-Line Monitoring of Responses to Nutrient Feed Additions by Multi-Frequency Permittivity Measurements in Fed-Batch Cultivations of CHO Cells. *Cytotechnology* **2010**, *62* (2), 121–132. <https://doi.org/10.1007/s10616-010-9267-z>.
- (103) Wasalathanthri, D. P.; Rehmann, M. S.; Song, Y.; Gu, Y.; Mi, L.; Shao, C.; Chemmalil, L.; Lee, J.; Ghose, S.; Borys, M. C.; et al. Technology Outlook for Real-Time Quality Attribute and Process Parameter Monitoring in Biopharmaceutical Development—A Review. *Biotechnology and Bioengineering*. John Wiley and Sons Inc October 1, 2020, pp 3182–3198. <https://doi.org/10.1002/bit.27461>.
- (104) Nguyen, B. N. B.; Ko, H.; Fisher, J. P. Tunable Osteogenic Differentiation of HMPCs in Tubular Perfusion System Bioreactor. *Biotechnol. Bioeng.* **2016**, *113* (8), 1805–1813.

- <https://doi.org/10.1002/bit.25929>.
- (105) Ball, O.; Nguyen, B. N. B.; Placone, J. K.; Fisher, J. P. 3D Printed Vascular Networks Enhance Viability in High-Volume Perfusion Bioreactor. *Ann. Biomed. Eng.* **2016**, *44* (12), 3435–3445. <https://doi.org/10.1007/s10439-016-1662-y>.
- (106) Stephenson, M.; Grayson, W. Recent Advances in Bioreactors for Cell-Based Therapies. *F1000Research* **2018**, *7*. <https://doi.org/10.12688/f1000research.12533.1>.
- (107) Bielser, J. M.; Wolf, M.; Souquet, J.; Broly, H.; Morbidelli, M. Perfusion Mammalian Cell Culture for Recombinant Protein Manufacturing – A Critical Review. *Biotechnology Advances*. Elsevier Inc. July 1, 2018, pp 1328–1340. <https://doi.org/10.1016/j.biotechadv.2018.04.011>.
- (108) Pattasseril, J.; Varadaraju, H.; Lock, L. T.; Rowley, J. A. Downstream technology landscape for large-scale therapeutic cell processing <https://bioprocessintl.com/upstream-processing/bioreactors/downstream-technology-landscape-for-large-scale-therapeutic-cell-processing-340981/>.
- (109) Heather Byer; Weihong Wang; Lana Mogilyanskiy. Mastering Cell Bank Production <https://www.biopharminternational.com/view/mastering-cell-bank-production> (accessed Jun 10, 2021).
- (110) Gebo, J. E. T.; Lau, A. F. Sterility Testing for Cellular Therapies: What Is the Role of the Clinical Microbiology Laboratory? *Journal of Clinical Microbiology*. American Society for Microbiology July 1, 2020. <https://doi.org/10.1128/JCM.01492-19>.
- (111) Barone, P. W.; Wiebe, M. E.; Leung, J. C.; Hussein, I. T. M.; Keumurian, F. J.; Bouressa, J.; Brussel, A.; Chen, D.; Chong, M.; Dehghani, H.; et al. Viral Contamination in Biologic Manufacture and Implications for Emerging Therapies. *Nat. Biotechnol.* **2020**, *38* (5), 1–10. <https://doi.org/10.1038/s41587-020-0507-2>.
- (112) Suvarna, K.; Lolas, A.; Patricia Hughes, M. S.; Friedman, R. L. MICROBIOLOGY-Case Studies of Microbial Contamination in Biologic Product Manufacturing. *Am. Pharm. Rev.* **2011**, *14* (1), 50.
- (113) Keane, J. T.; Ryan, D.; Gray, P. P. Effect of Shear Stress on Expression of a Recombinant Protein by Chinese Hamster Ovary Cells. *Biotechnol. Bioeng.* **2003**, *81* (2), 211–220. <https://doi.org/10.1002/bit.10472>.

- (114) Kim, B. J.; Oh, D. J.; Chang, H. N. Limited Use of Centritech Lab II Centrifuge in Perfusion Culture of RCHO Cells for the Production of Recombinant Antibody. *Biotechnol. Prog.* **2008**, *24* (1), 166–174. <https://doi.org/10.1021/bp070235f>.
- (115) Zhan, C.; Bidkhor, G.; Schwarz, H.; Malm, M.; Mebrahtu, A.; Field, R.; Sellick, C.; Hatton, D.; Varley, P.; Mardinoglu, A.; et al. Low Shear Stress Increases Recombinant Protein Production and High Shear Stress Increases Apoptosis in Human Cells. *iScience* **2020**, 101653. <https://doi.org/10.1016/j.isci.2020.101653>.
- (116) Clincke, M. F.; Mölleryd, C.; Zhang, Y.; Lindskog, E.; Walsh, K.; Chotteau, V. Very High Density of CHO Cells in Perfusion by ATF or TFF in WAVE BioreactorTM: Part I: Effect of the Cell Density on the Process. *Biotechnol. Prog.* **2013**, *29* (3), 754–767. <https://doi.org/10.1002/btpr.1704>.
- (117) Cunha, B.; Peixoto, C.; Silva, M. M.; Carrondo, M. J. T.; Serra, M.; Alves, P. M. Filtration Methodologies for the Clarification and Concentration of Human Mesenchymal Stem Cells. *J. Memb. Sci.* **2015**, *478*, 117–129. <https://doi.org/10.1016/j.memsci.2014.12.041>.
- (118) Schnitzler, A. C.; Verma, A.; Kehoe, D. E.; Jing, D.; Murrell, J. R.; Der, K. A.; Aysola, M.; Rapiejko, P. J.; Punreddy, S.; Rook, M. S. Bioprocessing of Human Mesenchymal Stem/Stromal Cells for Therapeutic Use: Current Technologies and Challenges. *Biochem. Eng. J.* **2016**, *108*, 3–13. <https://doi.org/10.1016/j.bej.2015.08.014>.
- (119) Nguyen, T.; Roddick, F. A.; Fan, L. Biofouling of Water Treatment Membranes: A Review of the Underlying Causes, Monitoring Techniques and Control Measures. *Membranes*. MDPI AG 2012, pp 804–840. <https://doi.org/10.3390/membranes2040804>.
- (120) BART, L.; BENJAMIN, R.-J.; ERIK, M.; MARK, B. Acoustic Perfusion Devices, 2020.
- (121) Nam, J.; Lim, H.; Kim, C.; Yoon Kang, J.; Shin, S. Density-Dependent Separation of Encapsulated Cells in a Microfluidic Channel by Using a Standing Surface Acoustic Wave. *Biomicrofluidics* **2012**, *6* (2), 024120. <https://doi.org/10.1063/1.4718719>.
- (122) Levison, P.; Elliott, A.; Wang, I.-K.; Collins, M. Acoustic Wave Separation – A Non-Filtration Approach for Continuous Clarification of Perfusion Cell Culture Prior to Capture Chromatography. *Integr. Contin. Biomanufacturing IV* **2019**.
- (123) Lipsitz, Y. Y.; Tonge, P. D.; Zandstra, P. W. Chemically Controlled Aggregation of

- Pluripotent Stem Cells. *Biotechnol. Bioeng.* **2018**, *115* (8), 2061–2066.
<https://doi.org/10.1002/bit.26719>.
- (124) Pohlscheidt, M.; Jacobs, M.; Wolf, S.; Thiele, J.; Jockwer, A.; Gabelsberger, J.; Jenzsch, M.; Tebbe, H.; Burg, J. Optimizing Capacity Utilization by Large Scale 3000 L Perfusion in Seed Train Bioreactors. *Biotechnol. Prog.* **2013**, *29* (1), 222–229.
<https://doi.org/10.1002/btpr.1672>.
- (125) Huang, D.; Man, J.; Jiang, D.; Zhao, J.; Xiang, N. Inertial Microfluidics: Recent Advances. *Electrophoresis* **2020**, *41* (24), 2166–2187.
<https://doi.org/10.1002/elps.202000134>.
- (126) Hansson, J.; Karlsson, J. M.; Haraldsson, T.; Brismar, H.; Van Der Wijngaart, W.; Russom, A. Inertial Microfluidics in Parallel Channels for High-Throughput Applications. *Lab Chip* **2012**, *12* (22), 4644–4650. <https://doi.org/10.1039/c2lc40241f>.
- (127) Miller, B.; Jimenez, M.; Bridle, H. Cascading and Parallelising Curvilinear Inertial Focusing Systems for High Volume, Wide Size Distribution, Separation and Concentration of Particles. *Sci. Rep.* **2016**, *6* (1), 1–8. <https://doi.org/10.1038/srep36386>.
- (128) Yin, L.; Yang, Z.; Wu, Y.; Denslin, V.; Yu, C. C.; Tee, C. A.; Lim, C. T.; Han, J.; Lee, E. H. Label-Free Separation of Mesenchymal Stem Cell Subpopulations with Distinct Differentiation Potencies and Paracrine Effects. *Biomaterials* **2020**, *240*, 119881.
<https://doi.org/10.1016/j.biomaterials.2020.119881>.
- (129) Kwon, T.; Prentice, H.; Oliveira, J. De; Madziva, N.; Warkiani, M. E.; Hamel, J. F. P.; Han, J. Microfluidic Cell Retention Device for Perfusion of Mammalian Suspension Culture. *Sci. Rep.* **2017**, *7* (1), 1–11. <https://doi.org/10.1038/s41598-017-06949-8>.
- (130) Matrosovich, M.; Herrler, G.; Klenk, H. D. Sialic Acid Receptors of Viruses. *Top. Curr. Chem.* **2015**, *367*, 1–28. https://doi.org/10.1007/128_2013_466.
- (131) Mascarenhas, J. X.; Korokhov, N.; Burger, L.; Kassim, A.; Tuter, J.; Miller, D.; Borgschulte, T.; George, H. J.; Chang, A.; Pintel, D. J.; et al. Genetic Engineering of CHO Cells for Viral Resistance to Minute Virus of Mice. *Biotechnol. Bioeng.* **2017**, *114* (3), 576–588. <https://doi.org/10.1002/bit.26186>.
- (132) Tasnim, H.; Fricke, G. M.; Byrum, J. R.; Sotiris, J. O.; Cannon, J. L.; Moses, M. E. Quantitative Measurement of Naïve T Cell Association with Dendritic Cells, FRCs, and

- Blood Vessels in Lymph Nodes. *Front. Immunol.* **2018**, 9 (JUL), 1571.
<https://doi.org/10.3389/fimmu.2018.01571>.
- (133) Weisbroth, S. H.; Kohn, D. F.; Boot, R. Bacterial, Mycoplasmal and Mycotic Infections. In *The Laboratory Rat*; Elsevier Inc., 2006; pp 339–421. <https://doi.org/10.1016/B978-012074903-4/50014-5>.
- (134) Ryu, W. S. *Molecular Virology of Human Pathogenic Viruses*; Elsevier Inc., 2016.
<https://doi.org/10.1016/c2013-0-15172-0>.
- (135) Goh, T. K. P.; Zhang, Z. Y.; Chen, A. K. L.; Reuveny, S.; Choolani, M.; Chan, J. K. Y.; Oh, S. K. W. Microcarrier Culture for Efficient Expansion and Osteogenic Differentiation of Human Fetal Mesenchymal Stem Cells. *Biores. Open Access* **2013**, 2 (2), 84–97.
<https://doi.org/10.1089/biores.2013.0001>.
- (136) Hong, J. S.; Azer, N.; Agarabi, C.; Fratz-Berilla, E. J. Primary Clarification of CHO Harvested Cell Culture Fluid Using an Acoustic Separator. *J. Vis. Exp.* **2020**, 2020 (159), 61161. <https://doi.org/10.3791/61161>.
- (137) Brandy Sargent. Clarification Using Acoustic Wave Separation Offers Advantages including -Continuous Process Solution <https://downstreamcolumn.com/clarification-using-acoustic-wave-separation-offers-advantages-including-continuous-process-solution/> (accessed Jun 8, 2021).